

11-2019

Integrating Geochronologic and Instrumental Approaches Across the Bengal Basin

Elizabeth L. Chamberlain

Steven L. Goodbred


Richard Hale

Michael S. Steckler

Jakob Willinga

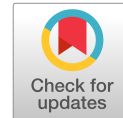
See next page for additional authors

Follow this and additional works at: https://digitalcommons.odu.edu/oeas_fac_pubs

 Part of the [Geology Commons](#), [Geomorphology Commons](#), [Geophysics and Seismology Commons](#), and the [Physical and Environmental Geography Commons](#)

Authors

Elizabeth L. Chamberlain, Steven L. Goodbred, Richard Hale, Michael S. Steckler, Jakob Willinga, and Carol Wilson



State of Science

Integrating geochronologic and instrumental approaches across the Bengal Basin

Elizabeth L. Chamberlain,^{1*} Steven L. Goodbred,¹ Richard Hale,² Michael S. Steckler,³ Jakob Wallinga⁴ and Carol Wilson⁵

¹ Department of Earth and Environmental Sciences, Vanderbilt University, Nashville, TN USA

² Department of Ocean, Earth, and Atmospheric Sciences, Old Dominion University, Norfolk, VA USA

³ Lamont-Doherty Earth Observatory of Columbia University, Palisades, NY USA

⁴ Netherlands Centre for Luminescence Dating & Soil Geography and Landscape Group, Wageningen University, Wageningen, The Netherlands

⁵ Department of Geology and Geophysics, Louisiana State University, Baton Rouge, LA USA

Received 1 March 2019; Revised 31 May 2019; Accepted 4 June 2019

*Correspondence to: Elizabeth L. Chamberlain, Department of Earth and Environmental Sciences, Vanderbilt University, 2305 W End Avenue, Nashville, TN 37203, USA.

E-mail: elizabeth.chamberlain@vanderbilt.edu

This is an open access article under the terms of the Creative Commons Attribution License, which permits use, distribution and reproduction in any medium, provided the original work is properly cited.

ESPL

Earth Surface Processes and Landforms

ABSTRACT: Constraining time is of critical importance to evaluating the rates and relative contributions of processes driving landscape change in sedimentary basins. The geomorphic character of the field setting guides the application of geochronologic or instrumental tools to this problem, because the viability of methods can be highly influenced by geomorphic attributes. For example, sediment yield and the linked potential for organic preservation may govern the usefulness of radiocarbon dating. Similarly, the rate of sediment transport from source to sink may determine the maturity and/or light exposure of mineral grains arriving in the delta and thus the feasibility of luminescence dating. Here, we explore the viability and quirks of dating and instrumental methods that have been applied in the Bengal Basin, and review the records that they have yielded. This immense, dynamic, and spatially variable system hosts the world's most inhabited delta. Outlining a framework for successful chronologic applications is thus of value to managing water and sediment resources for humans, here and in other populated deltas worldwide. Our review covers radiocarbon dating, luminescence dating, archaeological records and historical maps, short-lived radioisotopes, horizon markers and rod surface elevation tables, geodetic observations, and surface instrumentation. Combined, these tools can be used to reconstruct the history of the Bengal Basin from Late Pleistocene to present day. The growing variety and scope of Bengal Basin geochronology and instrumentation opens doors for research integrating basin processes across spatial and temporal scales. © 2019 The Authors. Earth Surface Processes and Landforms Published by John Wiley & Sons Ltd.

KEYWORDS: Ganges–Brahmaputra Delta; geochronology; river channel avulsion; relative sea-level rise and subsidence; sedimentary basin evolution

Introduction

Like sands through the neck of an hourglass, the fluvial and tidal channels of deltaic margins govern the transfer of sediment from large source terrains to their expansive ocean sinks. The movement of sediment through deltas is further dictated by the available accommodation created by relative sea-level rise (i.e. land surface subsidence and eustatic sea-level rise). Constraining the rates and timing of these processes through the application of geochronologic and instrumental tools is essential to determine the amount and distribution of available sediment, and also of tectonic, compactional, and marine controls that may generate space to capture it on the delta plain (e.g. Paola *et al.*, 2011; Allison *et al.*, 2016). In this sense, chronology is key to understanding basin evolution, and also to harnessing those processes

for nature-based solutions to delta management (e.g. Giosan *et al.*, 2014). Yet, chronologic constraints often prove to be the missing link in many studies, in part due to difficulties with identifying and applying suitable tools for challenging field settings.

The selection of appropriate geochronologic or instrumental tools for basin research requires careful consideration, as it is a function of the research question and geologic setting. Measured rates are known to vary by the time interval over which they are determined (Sadler, 1981). Each geochronometer or instrument also has limitations with regard to age range and material, and the availability of useful dating material can be highly site-specific. Applying chronology to deltas is especially complicated, due to the complexity imparted by intertwined river, tidal, and marine processes and their production of lithogenetically varied deposits that overlap in space and time. This complexity

may be further enhanced through the deformation of strata by seismic and tectonic processes.

This paper explores the topic of geochronologic and instrumental applications in deltas, with a focus on selecting methods appropriate to the geomorphologic attributes of the field site. Our investigation is framed in the immense and densely populated Bengal Basin (Figure 1A), and reviews the tools used therein to date and quantify sedimentary deposits of Pleistocene age to present day, and to reconstruct the fluvial and tectonic processes that govern sediment deposition. We discuss the attributes, shortcomings, and quirks of each method in the context of Bengal Basin geomorphology, the datasets which they have yielded, and the implications that may emerge from combined geochronologic and instrumental records. This novel perspective on chronology gives insights into the link between field setting and dating approach viability, thereby providing readers with the background needed to select appropriate methods for further advancing geochronologic and instrumental research into delta evolution. Such information is critical to establishing nature-based solutions to delta management.

The Bengal Basin

The Bengal Basin (Figure 1B) encompasses a vast area of 100,000 km², with the upper several hundred metres of sediment composed of a stacked patchwork of highstand deltas (Goodbred and Kuehl, 1999; Goodbred *et al.*, 2003; Pickering *et al.*, 2017) situated on a tectonically deforming platform (Steckler *et al.*, 2008, 2016). Of these deltas, the most recent is the up to 90 m thick Holocene sequence that contains deposits of the Ganges–Brahmaputra (G-B, sometimes referred to as the Ganges–Brahmaputra–Meghna) Delta and includes the veneer of a human-manipulated landscape (e.g. Auerbach *et al.*, 2015; Wilson *et al.*, 2017). The Holocene delta was constructed by sediment principally mobilized from the rapidly uplifting Himalayas and delivered to the delta plain via the presently 8 ± 4 and 10 ± 4 km wide channel belts of the respective

Ganges and Brahmaputra Rivers. Deposits from the last sea-level highstand (MIS 5e) outcrop as terraces in the upstream (fluvial) Bengal Basin (Pickering *et al.*, 2017). The Bengal Basin is exceptionally complex because it is shaped by rapidly migrating rivers (Sarker *et al.*, 2003) delivering an enormous and highly seasonal sediment load (Goodbred and Kuehl, 1999, 2000b; Rogers *et al.*, 2013), complex tidal signatures (Hale *et al.*, 2018), erosive yet constructive input by tropical cyclones (Darby *et al.*, 2016), seismic activity and tectonic deformation of the basement (Reitz *et al.*, 2015; Steckler *et al.*, 2016), and burgeoning human population pressure (Small and Nicholls, 2003; Brammer, 2014).

Establishing reliable chronology of landforms is a challenging task in general, especially in deltas, and most especially in the large, dynamic, and time-variable Bengal Basin. This is due in part to the enormous scale of the system and the significant number of unknowns (e.g. the challenge of putting a date into a solid geologic context or designing a sampling strategy). Large numbers of dated samples or instrumental measurements are needed to truly capture the Bengal Basin's processes over its immense spatial and depth scales. Such an approach can be quite costly and was likely beyond the means of the earliest studies employing chronology. Furthermore, there are significant logistical and travel limitations to spatially canvassing the Bengal Basin; anecdotally these include slow transportation, sporadic lodging, lack of road connectivity, and as reported by Allison and Kepple (2001), the 'presence of tigers'.

The earliest chronologic framework of the Bengal Basin emerged roughly half a century ago, based primarily on historical records, geomorphic/stratigraphic principles, and a few radiocarbon ages (Morgan and McIntire, 1959; Coleman, 1969). This sketch has been refined in recent decades through chronologies derived from radiocarbon dating (e.g. Umitsu, 1993; Stanley and Hait, 2000; Goodbred and Kuehl, 2000a; Suckow *et al.*, 2001; Allison *et al.*, 2003; Pickering *et al.*, 2014; Sincavage *et al.*, 2018), short-lived radioisotopes (e.g. Goodbred and Kuehl, 1998; Allison and Kepple, 2001; Suckow *et al.*, 2001; Rogers *et al.*, 2013), and most recently, luminescence dating (e.g. McArthur *et al.*, 2008; Weinman *et al.*, 2008; Chamberlain

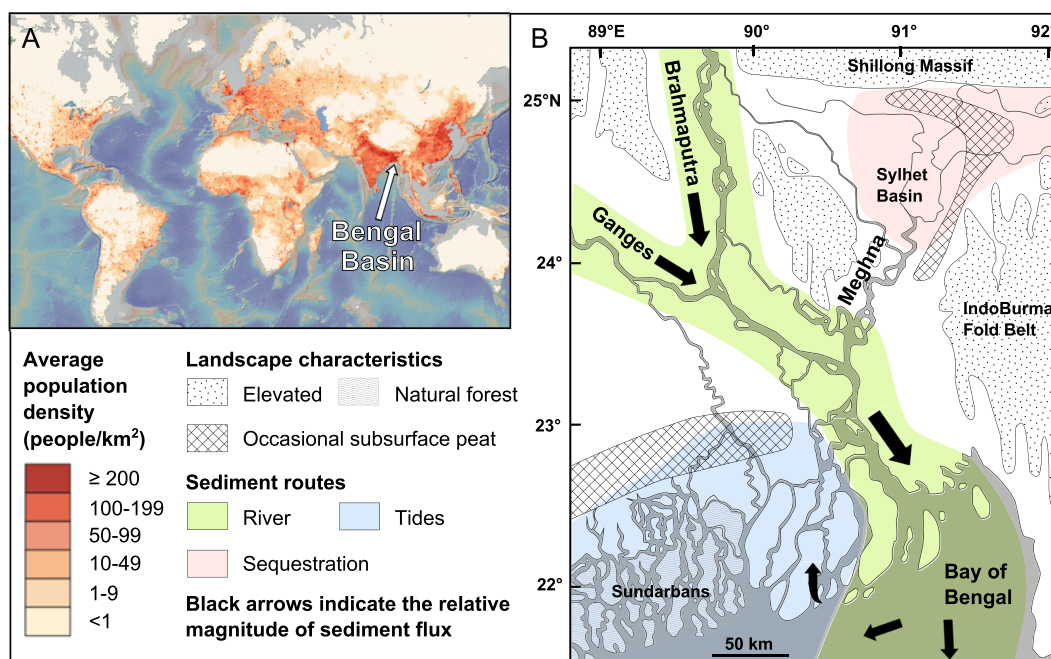


Figure 1. (A) The Bengal basin hosts one of the most densely populated landscapes on Earth (image modified from CIESIN, 2005), with a mean population density of approximately 1100 people km⁻² (Small and Nicholls, 2003). (B) The geomorphology of the Bengal Basin is complex. Here, major rivers and tidal channels, elevated features, the natural Sundarbans forest, regions which may contain peat basin deposits, sediment routes, and relative magnitudes of annual sediment flux (see Goodbred and Kuehl, 1999; Wilson and Goodbred, 2015) are shown. [Colour figure can be viewed at wileyonlinelibrary.com]

et al., 2017 ; Pickering et al., 2017) and satellite imagery (e.g. Higgins et al., 2014 ; Wilson et al., 2017 ; Dixon et al., 2018). Given the perspective of time and scientific advancement, a review by practicing geochronologists of published geochronologic datasets is important for scrutinizing the present record of the Bengal Basin, because unsuitable approaches and/or geochronologic records can become canonized by repetition. Furthermore, ages are only as good as the geologic framework into which they are placed. In contrast, methodologically correct and geologically robust chronologic data have an outstanding capacity to inform knowledge of the histories and processes of evolving landscapes.

Here we review and summarize the advancement of geochronologic and instrumental methods for determining the rates and patterns of the intermingled processes that shape the Bengal Basin (Figure 2). Our review first covers broadly applicable methods, including the classical approach of radiocarbon dating and the developing suite of luminescence dating tools. These geochronometers can be applied to constrain and quantify a wide range of processes in the delta, such as subsidence (e.g. Grall et al., 2018), accretion (e.g. Chamberlain et al., 2017), and determining the timing and pathways of active river channels (e.g. Allison et al., 2003 ; Sincavage et al., 2018). We then focus on methods that have been used to specifically capture subsidence (e.g. GNSS, archaeological records, tide gauges, InSAR, and RSETs; Steckler et al., 2010; Sarker et al., 2012; Pethick and Orford, 2013; Higgins et al., 2014; Wilson et al., 2018) and sediment accretion (e.g. radionuclides and RSETs; Goodbred and Kuehl, 1998; Bomer et al., 2017) in the Bengal Basin. Maps and satellite imagery (e.g. Addams, 1919 ; Wilson et al., 2017) can be used to assess changes in the planform of the delta (e.g. river and tidal channel pathways or coastline evolution). Finally, we discuss instrumental methods for determining water movement in the delta (e.g. tide gauges and acoustic Doppler current profiler; Singh, 2002; Hale et al., 2018; Bain et al., In press; Hale et al., 2019). Combined, these tools cover a diverse range of timescales and temporal resolutions, and enable 'rating and dating' of the Bengal Basin (Figure 2).

Radiocarbon Dating

Radiocarbon dating (Table I) is a classic dating approach that has informed some of the first absolute, prehistoric

chronologies of deltas worldwide (e.g. Fisk, 1952 ; Berendsen, 1984). This method makes use of the proportion of the ^{14}C isotope that is fixed in plants or animals at the time of their death and decays at a half-life of 5730 years. A radiocarbon age is obtained by measuring the ratio of radioactive (^{14}C) to stable (^{12}C) carbon in organic remains and calculating the decay time needed to reach that proportion from the original, which is then calibrated for atmospheric variations in ^{14}C (e.g. Ramsey, 1995). With direct ion counts obtained by accelerator mass spectrometry, radiocarbon can be measured to ~8 half-lives, giving a theoretical maximum age of ~45 to 50 thousand years (ka). Although calibration is possible up to 50 ka cal BP (Reimer et al., 2013), dating of samples > 26 ka cal BP may be problematic in practice as minor contaminations may induce large age offsets, as is evident from deviating attempts to establish calibration curves (Van der Plicht et al., 2004), and published examples of radiocarbon age underestimation (e.g. Briant and Bateman, 2009 ; Busschers et al., 2014 ; Briant et al., 2018).

Introduced in the 1940s (Anderson et al., 1947; Arnold and Libby, 1949), the earliest radiocarbon approaches required beta counting of the radioactive decay emitted from large amounts of bulk organic material. This sometimes overestimated age by thousands of years when the bulk material was not carefully selected (e.g. Frazier, 1967), although fairly accurate chronologies could be obtained through beta counting of rigorously sampled bulk material (e.g. McFarlan, 1961; Berendsen, 1984). The advancement of accelerator mass spectrometry allows for measurement of minute organic remains (e.g. single seed pods or foraminifera shells), which are more likely to be directly related to the geologic event of interest and therefore yield more accurate ages (e.g. Törnqvist et al., 1996). The earliest radiocarbon records, while state-of-the-art at their publication time, should therefore be regarded with caution. Radiocarbon dating of very young (less than ~300 years) material is generally not reliable due to the high anthropogenic input of carbon to the atmosphere (e.g. see Levin and Hesshaimer, 2000), although there has been some recent progress on developing radiocarbon approaches for the past few centuries, including 'post-bomb' calibration (see Törnqvist et al., 2015). Altogether, this means that radiocarbon dating can presently yield reliable ages within the range of 30,000–300 years, provided that suitable organic material is measured.

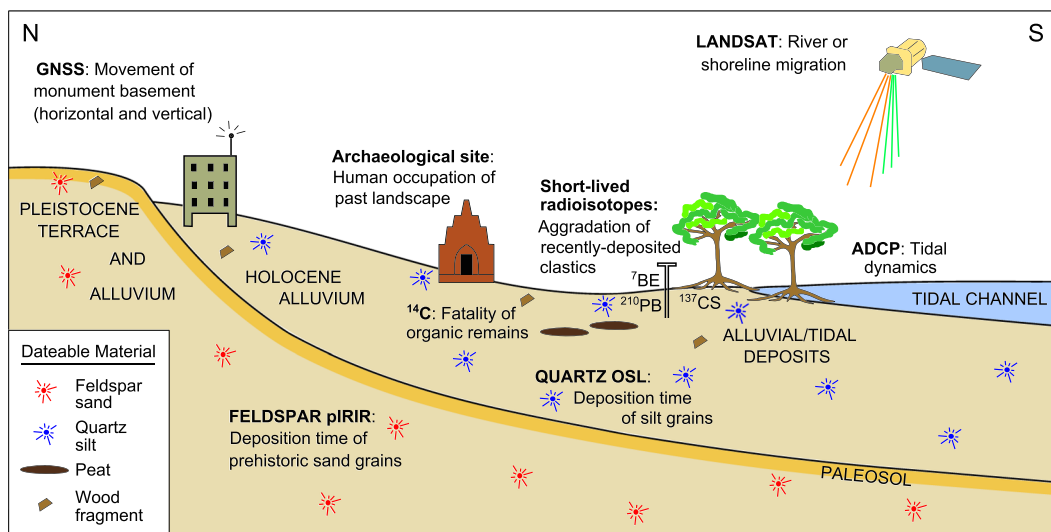


Figure 2. Integrating geochronologic and instrumental methods across a deltaic landscape. Various methods (bold text) can be applied to different regions and materials, to measure processes acting over a range of time and spatial scales. Research may be further enhanced by data obtained from InSAR, RSETs, and historical maps (not pictured here). Together, this yields a holistic view of delta evolution. [Colour figure can be viewed at wileyonlinelibrary.com]

Table 1. Geochronologic and instrumental methods and their age ranges of application in the Bengal Basin, timescale of resolution, requirements, and selected references. Note that age ranges are highly variable and can be different in other geologic settings and systems

Method	Age range		Timescale of resolution	Requirements	Selected Bengal Basin references
	Confident	Perhaps possible			
<i>Long-term methods</i>					
Radiocarbon dating	30 000–300 years	45 000–30 000 years	10^3 – 10^1	Preserved organic material that died relevant to the event of interest	Goodbred and Keuhl (2000a), Sincavage <i>et al.</i> (2018), Grall <i>et al.</i> (2018)
Luminescence dating – quartz OSL	25 000 years–present	—	10^3 – 10^1	Preservation of sensitive quartz grains, sufficient resetting of the OSL signal by light exposure	Chamberlain <i>et al.</i> (2017)
Luminescence dating – feldspar IRSL/pIRIR	>500 000–11 000 years	11 000–present	10^5 – 10^4	Preservation of feldspar grains, sufficient resetting of the IRSL or pIRIR signal by light exposure, a-thermal stability	Pickering <i>et al.</i> (2017)
Human history and maps	1600 years–present	6000–1600 years	10^2 – 10^{-1}	Written records (text or maps) documenting natural events and/or describing archaeological sites	Addams Williams (1919), Jahan (2010), Sarker <i>et al.</i> (2012), Hanebuth <i>et al.</i> (2013), Wilson <i>et al.</i> (2017)
<i>Short-lived methods</i>					
Atmospheric fallout radionuclides	100–0.5 years	—	10^1 – 10^{-3}	Low bioturbation and/or sediment mixing	Goodbred and Kuehl (1998), Allison and Kepple (2001), Rogers <i>et al.</i> (2013)
Horizon markers	5 years–present	10 years–present	10^{-1} – 10^{-2}	Lack of bioturbation, erosion, and/or human disturbance of the marker	Rogers <i>et al.</i> (2013), Rogers and Overeem (2017)
RSETs	5 years–present	—	10^{-1} – 10^{-2}	Stable benchmark driven to depth of refusal, seasonal visits for measurement	Bomer <i>et al.</i> (2017), Wilson <i>et al.</i> (2018)
<i>Geodetic observations</i>					
GNSS	15–3 years	—	10^{-1} – 10^{-3}	Fixed antennas communicating with satellites	Steckler <i>et al.</i> (2010), Vernant <i>et al.</i> (2014), Reitz <i>et al.</i> (2015), Steckler <i>et al.</i> (2016)
InSAR	5 years–present	—	10^1 – 10^{-1}	Image coherency, which can be hindered by water or vegetation	Higgins <i>et al.</i> (2014)
<i>Surface instrumentation</i>					
Tide gauges	60 years–present	—	10^1 – 10^{-5}	Reliable benchmark, good data management	Singh (2002), Pethick and Orford (2013), Hale <i>et al.</i> (2018)
ADCP	3 years–present	—	10^{-1} – 10^{-5}	Understanding of channel areas and velocities, no disturbance/disappearance of deployed instruments	Hale <i>et al.</i> (2018), Bain <i>et al.</i> , (In press), Hale <i>et al.</i> , (2019)

Geomorphic constraints on peat

In the Bengal Basin, the *in-situ* organic material (e.g. peat) that is most preferred for radiocarbon dating is notably limited in the Holocene package of the G-B Delta (Goodbred and Kuehl, 1999). As such, only a relatively small number of ages obtained from peat have been reported, and these are mostly limited to shallow (<10 m), Middle to Late Holocene-age deposits from localized basins in the central delta plain (Umitsu, 1993; Goodbred and Kuehl, 2000a; Allison *et al.*, 2003; Brammer, 2012).

The low formation and preservation of peat in the Bengal Basin is a direct consequence of the system's sedimentary processes and environmental conditions. Three principal factors play a role: (i) a lack of available accommodation due to the high sediment yield (Chamberlain *et al.*, 2017); (ii) remineralization and flushing under the highly seasonal climate (Allison *et al.*, 2003); and (iii) a lack of preservation due to laterally mobile channel belts in upstream regions of the delta (Wilson and Goodbred, 2015). Foremost, the widespread, seasonal deposition of siliciclastic sediment limits the concentrated accumulation of organic matter. This low organic-to-clastic ratio is a function of sediment yield (Figure 3), because mineral sediment aggrades more rapidly and is therefore more efficient at filling accommodation than organic deposits (i.e. peat) that grow slowly *in situ* (Chamberlain *et al.*, 2017). Overall, the sediment yield of the Bengal Basin throughout the Holocene has been exceptionally high relative to many deltas (Goodbred and Kuehl, 2000a), because it is fed by two of the rivers draining the rapidly uplifting Himalayas and the powerful erosive and transport engine of the Southeast Asian Monsoon (Goodbred and Kuehl, 2000b).

Furthermore, the regular input of sediment coupled with the annual dry season limits the extent of perennially flooded basins where organic matter is best preserved. Thus, most organic production is seasonally remineralized in oxidizing, vadose soils. Finally, the large, laterally mobile channel belts of the main rivers effectively rework shallow stratigraphy across the Bengal Basin (Wilson and Goodbred, 2015), so even where

peats form, they are rarely preserved within the long-term stratigraphy.

As a consequence of these factors, the formation of peats is largely restricted to distal, sediment-starved areas of the delta, found locally within the Sylhet Basin and the central delta plain (Figure 1). The 'peat basins' of the central delta plain (Brammer, 2012; Wilson and Goodbred, 2015) contain alternating layers of peat and clay-rich muds, restricted to the upper 3–6 m of stratigraphy (Azeem and Khalequzzaman, 1994). These near-surface deposits in the lower delta have principally dated to 1–6 ka, indicating that the basins have received limited sediment input and burial during that time (Khan and Islam, 2008). The deficit of sediment in these basins is a consequence of their location at the distal reaches downstream of the Ganges' ephemeral distributaries and upstream of the major coastal tide channels. Thus, without the main rivers having occupied this area for the last several thousand years, peats have formed and been preserved over this time. However, a future avulsion of the main channels to these areas would rework and remove most of the shallow organic-rich deposits. Additionally, many of these basins have been drained or dredged for agriculture and aquaculture production in recent decades, thus much of the natural 'peat basins' of historical lore have been lost. Finally, it is worth noting that peat formation and organic preservation is even rare in the Sundarbans coastal mangrove forest, which contrasts with the organic-rich deposits associated with some other mangrove settings (e.g. Woodroffe *et al.*, 2016). In the Sundarbans, this lack of organics is due to active tidal sediment deposition and bioturbation (Rogers *et al.*, 2013; Gain and Das, 2014).

Applications to refractory remains

In the absence of widespread *in-situ* organic markers such as peats, Bengal Basin radiocarbon records have been obtained from particles of other organisms including carbonate shells (e.g. Hait *et al.*, 1996; Suckow *et al.*, 2001), plant material (wood, grass, leaves) embedded within riverine deposits (Allison *et al.*, 2003; Pickering *et al.*, 2014; Grall *et al.*, 2018; Sincavage *et al.*, 2018), and even a crab claw (Allison *et al.*, 2003). The association of such material to the event or deposits of interest is tenuous, because these more refractory remains may be much older than the sediment in which they are encased (Schiffer, 1986). Shells of marine or estuarine origin are also affected by the initial $^{14}\text{C}/^{12}\text{C}$ ratio fixed in these organisms, which is a function of the local water source(s) and chemistry where they lived. This reservoir effect is often poorly constrained, especially in estuarine settings, and may decrease the precision of results or lead to inverted and anomalous ages (e.g. Törnqvist *et al.*, 2015). Furthermore, many of the radiocarbon records from the G-B Delta consist of relatively few ages dispersed across wide geographic ranges (e.g. Allison *et al.*, 2003). It is difficult to validate such radiocarbon records due to the lack of independent chronology and too few ages to check for internal consistency (i.e. stratigraphic correctness).

A large collection ($n = 198$) of terrestrial radiocarbon ages, primarily of wood fragments, yielded internally consistent ages for Bengal Basin sedimentary deposits (Pickering *et al.*, 2014; Grall *et al.*, 2018; Sincavage *et al.*, 2018), suggesting that radiocarbon can be a viable dating approach for the Bengal Basin despite the lack of a known, direct relationship between these organic fragments and the river and floodplain deposits in which they were embedded. This finding supports that previous datasets of small numbers of radiocarbon ages obtained from similar material (i.e. macro-particles of terrestrial plant remains) are likely to be trustworthy (e.g. see Allison *et al.*, 2003, table

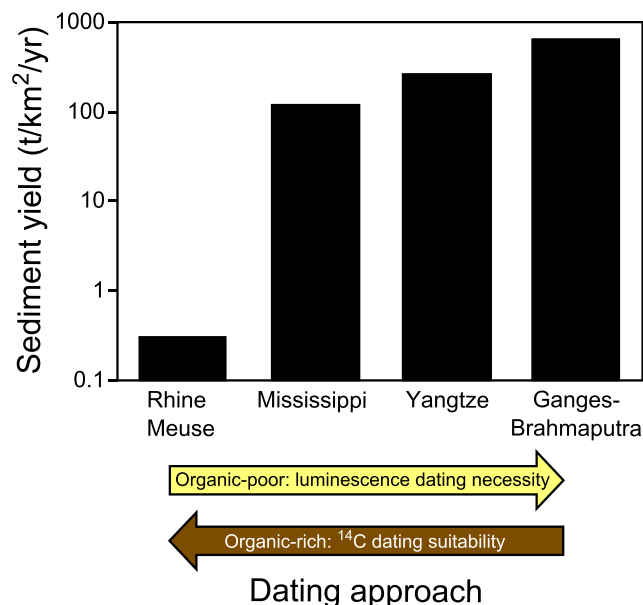


Figure 3. The selection of an approach to dating deltaic deposits is a function of the organic-to-clastic ratio of the stratigraphic record, which is primarily defined by sediment yield. Adapted from Chamberlain *et al.* (2017), with sediment yield values from Milliman and Farnsworth (2013). [Colour figure can be viewed at wileyonlinelibrary.com]

1). The success of this approach may be due in part to the low delta-wide preservation of organic material. Wood fragments in the Bengal Basin appear to be generally contemporaneous to the sediments in which they are encased, and therefore contain a representative $^{14}\text{C}/^{12}\text{C}$ ratio at the time of deposition. They are not likely mobilized by river incision into older ^{14}C -deficient organic deposits, as previously proposed (Stanley and Hait, 2000), although the coastward delivery of ^{14}C -depleted material by rivers (Raymond and Bauer, 2001) remains a reasonable mechanism of age overestimation in other, more organic-rich deltas (e.g. Geyh *et al.*, 1983). In other words, the unavailability of organics in the delta's stratigraphic record both hinders and helps radiocarbon dating, by limiting the dateable material yet also limiting old-carbon contamination.

Unlike peat beds which grow in association with the local coeval water table and/or sea level, and therefore can serve as precise markers of hydrologic conditions (e.g. Törnqvist *et al.*, 2004), the immediate relationship of wood fragments to depth and hydrology (sea level, water table, and/or river bed depth) is uncertain. Thus, radiocarbon ages of particulate organic matter collected from fluvial sands may have been deposited on the channel bed or within local scours that are 15 m or more below the local river surface elevation (Grall *et al.*, 2018). We speculate that much of the wood preserved in fluvial sands of the Bengal Basin is related to lateral channel erosion and bank collapse, which can rapidly bury bank-edge vegetation before it is remineralized, effectively sequestering that material to the channel base.

Luminescence Dating

In his fundamental paper on the Brahmaputra River, Coleman (1969) provided a geochronologic sketch of the G-B Delta, noting: 'Time relationships of the various units are tentative... Until a suitable dating method is established, this problem will remain unsolved'. The introduction of optically stimulated luminescence dating to geoscience research (Huntley *et al.*, 1985), plus subsequent methodological (e.g. Hütt *et al.*, 1988; Murray and Wintle, 2000, 2003; Thomsen *et al.*, 2008) and statistical improvements (e.g. Galbraith *et al.*, 1999; Cunningham and Wallinga, 2010, 2012) of recent decades, now make it possible to directly date the deposition of riverine clastic sediments, thereby providing a means to fill the void recognized by Coleman (1969).

Luminescence dating (Table I) includes a suite of sub-methods that estimate the burial age of sediment from trapped charge that accumulates in mineral (e.g. quartz; Huntley *et al.*, 1985 or feldspar; Hütt *et al.*, 1988) grains when they are removed from light. During transit in a river, marine or tidal environment, the trapped charge may be zeroed ('reset', 'bleached') by sunlight exposure as grains experience temporary storage in floodplains or bars (e.g. Stokes *et al.*, 2001) or as they approach the water surface through turbulence (e.g. Gemmill, 1988).

Upon burial, the mineral grains are exposed to ionizing radiation from the decay of naturally occurring radioisotopes (^{40}K ; thorium and uranium decay chains) within the surrounding sediment matrix, as well as a typically minor component of radiation from cosmogenic rays and internal mineral inclusions (e.g. see Durcan *et al.*, 2015). Absorption of this radiation causes charge to become trapped within the mineral crystal lattice. Following careful sampling and processing to preserve the light-sensitive signal(s) of interest, the grains are stimulated in a laboratory by heat (thermoluminescence), blue light (optically stimulated luminescence, OSL), or infrared light (infrared stimulated luminescence, IRSL) to release the trapped charge and measure

the evicted luminescence signal that results. Through comparison with luminescence signals induced by laboratory charging from calibrated radiation sources, this yields an estimate of the total radiation dose received since burial, or the 'paleodose' of the sample. A luminescence age is calculated by dividing the paleodose by the yearly radiation dose ('dose rate'), estimated from radionuclide concentrations of the sample and surrounding bulk sediment and cosmogenic dosing, and taking into account attenuation factors (e.g. water content, grain size).

In addition to allowing for direct dating of the burial of riverine, tidal, and coastal deposits, the suite of sub-methods that make up luminescence dating offer the most versatile delta geochronologic approach in terms of timescale. Dating protocols that target the OSL signal arising from quartz can yield accurate ages for deposits from under a decade (Madsen and Murray, 2009), to upwards of a few hundred thousand years (Schokker *et al.*, 2005). Protocols targeting feldspar signals can reach beyond 500 000 years (see Wallinga and Cunningham, 2015 for a review of luminescence age ranges and uncertainties). The upper age limit of luminescence dating is highly variable by geography, regardless of the selected mineral and protocol, because it is set by the dose rate and saturation behaviour of the grains (see Wintle and Murray, 2006).

There are three primary criteria for luminescence dating of sedimentary deposits: (i) the mineral is luminescence sensitive, meaning it produces a luminescent signal after ionizing radiation exposure; (ii) at least some grains within the sample have had the luminescence signal of interest completely reset prior to burial; and (iii) the signal of interest is stable with time (Chamberlain, 2018). Quartz OSL offers the most readily reset and stable luminescence signal (Godfrey-Smith *et al.*, 1988; Wallinga, 2002). However, quartz is not ubiquitously sensitive. Rather, quartz sediments gain sensitivity with repeated episodes of luminescence signal accumulation and bleaching (Pietsch *et al.*, 2008), and are often poorly sensitized in young quartz grains sourced from igneous or metamorphic bedrock (Guralnik *et al.*, 2015). Feldspar IRSL is more ubiquitously sensitive (e.g. Reimann *et al.*, 2017). Yet, the feldspar IRSL signal is a-thermally unstable, that is, it loses charge ('fades') with time (Spooner, 1994). Measurement of the feldspar IRSL signal at elevated temperatures following a lower-temperature IRSL measurement (known as post-infrared infrared stimulated luminescence, or pIRIR) targets more stable yet less readily reset signals (Thomsen *et al.*, 2008; Kars *et al.*, 2014).

Sand-sized particles are typically preferred for optically stimulated luminescence dating of fluvial deposits because these allow for the measurement of small aliquots containing a few or even individual grains (Wallinga, 2002). This can be valuable for obtaining an accurate paleodose through statistical approaches when some but not all sand grains in a sample have been reset prior to deposition (Galbraith *et al.*, 1999). By contrast, measurement of silt yields an average paleodose which may arise from over 1 million grains per aliquot (e.g. Duller, 2008). Therefore, luminescence dating of silt is only viable if the overwhelming majority of silt grains within the sample have been reset prior to deposition. Finally, as with most geochronologic methods, care should be taken to obtain representative samples. For luminescence dating, this often (but not always, see Reimann *et al.*, 2017) means avoiding bioturbated material, which may include very shallow sediments (e.g. <1 m depth) or coastal/estuarine muds in the G-B Delta.

Quartz OSL applications

Luminescence dating has seen limited application in the Bengal Basin at present, with few published studies employing

the technique (see McArthur *et al.*, 2008; Weinman *et al.*, 2008; Chamberlain *et al.*, 2017; Pickering *et al.*, 2017). This is due in part to the relative newness of this method, but perhaps more importantly, to the significant obstacles presented by the geologic setting of the Bengal Basin. The Himalaya-derived quartz sand is poorly sensitized (Jaiswal *et al.*, 2008) when it enters the delta via the Ganges and Brahmaputra Rivers, and opportunities for in-delta sensitization are limited by rapid source-to-sink transport (Goodbred, 2003). A basin-wide assessment of the sensitivity and bleaching of multiple luminescence signals by Chamberlain *et al.* (2017), informed by 13 samples representing inland and coastal deposits of the three primary rivers (Ganges, Brahmaputra, and Meghna) and mixed-river source deposits, confirmed that most regions of the G-B Delta possess insensitive quartz sand that is not suitable for luminescence dating (Figure 4A). Surprisingly, sedimentary deposits in the northeast corner of the delta were found to contain sensitive quartz sand (Chamberlain *et al.*, 2017). This was attributed to the unique tectonic and fluvial history of the region, where the tectonically uplifted ancient (up to Paleogene-aged) sedimentary deposits of the paleo-Bengal Delta form the present-day Indo-Burman Fold Belt (Steckler *et al.*, 2008) (Figure 1). Unlike sediments produced from igneous and metamorphic bedrock, those sourced from sedimentary rock are more likely to contain sensitive quartz (Sohbati *et al.*, 2012). Yet, the sensitive quartz sand of this locality remains largely sequestered within the hydrologically disconnected Sylhet Basin (Figure 1), and the population that does escape via the Meghna River is highly diluted when it joins the Brahmaputra River system (Padma River) and coastal/tidal sites downstream by insensitive quartz sand of the larger rivers (Chamberlain *et al.*, 2017). Notably, quartz sand OSL ages have been obtained from the alluvial floodplain of western India (Jain and Tandon, 2003; Jain *et al.*, 2005), and from the Ganga Plain (although low quartz sensitivity was observed; Ray and Srivastava, 2010), suggesting that a small yet dateable population of quartz sand may reach the delta via the Ganges River, although this has not yet been identified.

Despite the limitations of quartz sand, quartz silt isolated from sedimentary deposits of the Bengal Basin possesses suitable luminescence properties, including acceptable sensitivity and pre-depositional resetting (Figure 4B), and was shown to yield ages consistent with independent chronologies (Chamberlain *et al.*, 2017). Sufficient bleaching of quartz silt has been identified in other large deltas, including those of the Mississippi (Shen *et al.*, 2015) and Yangtze Rivers (Sugisaki *et al.*, 2015; Gao *et al.*, 2018; Nian *et al.*, 2018). This supports recent observations,

drawn from the Mississippi system, that turbulence within the water column of large rivers may play an important role in bleaching of suspended particles during fluvial transport (Chamberlain and Wallinga, 2019). However, the utility of this discovery in the Bengal Basin may be limited by the sand-dominated nature of its deposits, especially in the upstream reaches of the fluvial delta (Wilson and Goodbred, 2015), and by a quartz silt upper age limit of ~25 000 years set by the early saturation behaviour of the grains and high dose rates of G-B muds averaging ~4.1 Gy ka⁻¹ (Chamberlain *et al.*, 2017).

Feldspar IRSL applications

Feldspar extends the age range of luminescence dating, and was used by Pickering *et al.* (2017) to estimate the age of three samples obtained from terrace deposits of the paleo-Brahmaputra River in the upper Bengal Basin. The dated deposits were known to be pre-Holocene in age due to their stratigraphic position below radiocarbon-dated Holocene sediments, and/or extensive weathering and high degree of compaction at nearby exposed sites (Pickering *et al.*, 2014). Measurement of small-diameter, multi-grain feldspar aliquots using a pIRIR-290 protocol (Thiel *et al.*, 2011) with a fading correction following Huntley and Lamothe (2001) extrapolating 2–3% fading per decade yielded ages upwards of 100 000 years (Pickering *et al.*, 2017). It is noteworthy that such a fading correction may overestimate fading of old samples like these, which are in the higher portion of the saturation curve (Kars *et al.*, 2008). However, both fading-corrected and uncorrected ages were reported and these agreed within uncertainty (Pickering *et al.*, 2017). A dose of 25 Gy was subtracted from the paleodose of each sample to account for poor bleaching of the pIRIR-290 signal; such a correction is not atypical for luminescence dating of high-temperature feldspar signals (e.g. Joordens *et al.*, 2015). With reported dose rates of 2.3–3.6 Gy ka⁻¹ (Pickering *et al.*, 2014), this bleaching correction corresponds to ~7000 to 11 000 years of residual dose.

No Holocene pIRIR ages have yet been reported for the Bengal Basin, and a multi-thousand-year correction for poor bleaching like that applied by Pickering *et al.* (2014) would disqualify results for Holocene-aged samples. Nevertheless, pIRIR dating may still be possible using lower temperatures for pIRIR stimulations (Madsen *et al.*, 2011; Reimann *et al.*, 2011), combined with single-grain measurements (e.g. Brill *et al.*, 2018) or fading-corrected IRSL. Although correction for anomalous

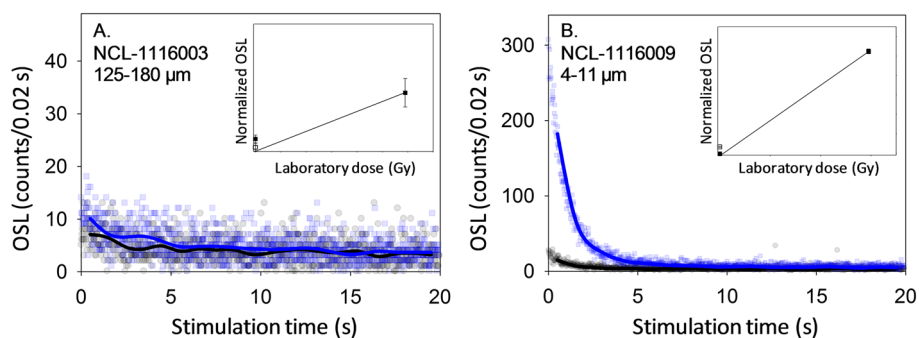


Figure 4. Typical quartz OSL responses of (A) sand, and (B) fine silt isolated from young (<45 years) G-B Delta deposits, including the luminescence decay curves and dose–response measurements (inset). For decay curves, the natural signal is shown in black and a regenerative signal (A: 5.9 Gy, B: 2.95 Gy) is shown in blue. (A) Quartz sand generally has low OSL sensitivity, indicated by low OSL counts within the first few seconds of stimulation, making it unsuitable for luminescence dating. The low natural signal yet high regenerative signal of (B) quartz silt indicates that this fraction is both well bleached and sensitive, making it suitable for luminescence dating. See Chamberlain *et al.* (2017) for full details of the samples. [Colour figure can be viewed at wileyonlinelibrary.com]

fading will be needed (Auclair *et al.*, 2003), the better bleachability of such signals compared to pIRIR measured at 290 °C (Kars *et al.*, 2014) provides a reasonable compromise. As a large fraction of feldspar grains often produce a measurable luminescence signal, single-grain pIRIR dating of feldspar may allow the use of advanced statistical methods to select the best-bleached grains. To the best of our knowledge, single-grain pIRIR dating has not yet been attempted for G-B Delta deposits.

Human History

Deltas are living landscapes, where high bioproductivity, access to waterway transportation, and resource availability drive high human population density. These rich ecotomes also often serve as ‘cradles of civilization’ (e.g. Day *et al.*, 2007), and thereby offer longstanding human records in the form of archaeological sites and historical maps or other written documents. The human record can inform knowledge of deltaic evolution over the past few thousand years, and may influence the scope of questions we ask as scientists. For example, high-resolution historical records of the Rhine Meuse Delta enable testing new geochronologic approaches against known-age deposits (e.g. Cunningham and Wallinga, 2010). Similarly, the relatively rapid avulsion timescale plus lengthy historical record of the Yellow River Delta (Saito *et al.*, 2000) has minimized the need for research on recent lobe (subdelta) chronology and allowed contemporary research to address other questions such as the mechanisms of avulsion setup (e.g. Ganti *et al.*, 2014). Meanwhile, lobe chronology and growth history remain a current line of inquiry in deltas with millennial-timescale avulsions and/or lower-resolution historical records (e.g. Hijma *et al.*, 2017; Chamberlain *et al.*, 2018), including the G-B Delta (e.g. Allison *et al.*, 2003).

Archaeological sites

At present, the Bengal Basin historical archive (Table I, Figure 5) is relatively short and low-resolution compared with some other Asian deltas such as the Yellow River Delta, but still more informative than records of more remote tropical deltas such as the Fly River Delta of Papua New Guinea. While the Bengal Basin archaeological record extends to the second millennium BCE, information is limited until the 4th century CE, when Bengal came under Gupta rule. Still, much of the eastern delta remained sparsely populated until the historically recorded ‘avulsion’ of the Ganges from the Hooghly channel to the present Padma channel over the 16 to 19th centuries (Eaton, 1993). Many pre-historic archaeological sites have only been relatively dated by typology of artefacts, and lack absolute chronologies (Rajaguru *et al.*, 2011).

There has been limited use of archaeological sites for geologic investigations in the Bengal Basin. Rajaguru *et al.* (2011) investigated the stratigraphic relationship of archaeological horizons to natural flood deposits at three sites in West Bengal, yet had little absolute chronology. The authors identified the potential of luminescence dating to directly link archaeological sites to processes of landscape evolution, including paleochannel activity (Rajaguru *et al.*, 2011). Wari-Bateshwar (Figure 5), near Narsingdi (Jahan, 2010), arose around 450 BCE and declined during the 7th century CE, likely in concert with avulsions of Old Brahmaputra River and the changing position of its confluence with the Meghna River (Figure 6A). Hanebuth *et al.* (2013) estimated coastal subsidence by dating a 300-year-old salt-making facility (Figure 5) uncovered by Cyclone Sidr in the Sundarbans. The age of the

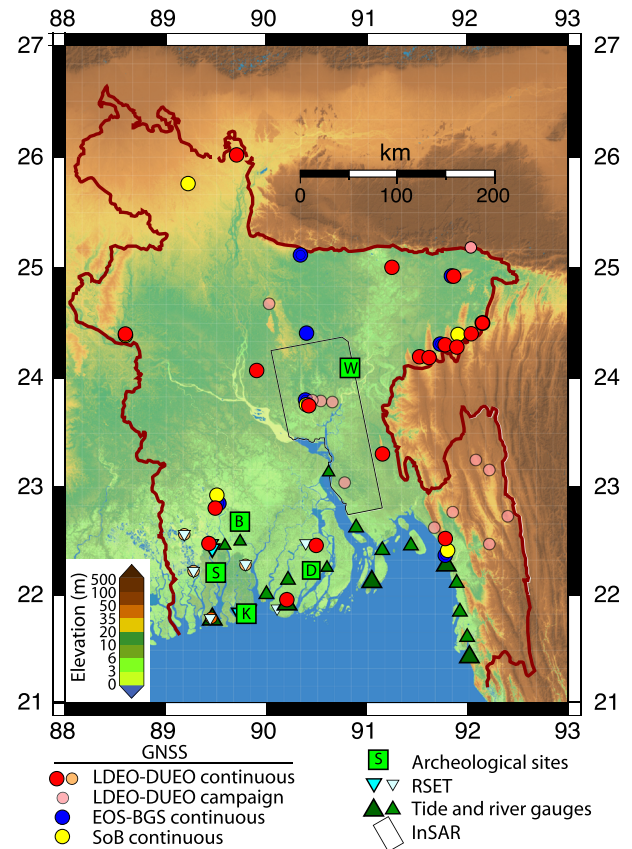


Figure 5. Map showing the location of GNSS and RSET installations, InSAR measurements, and archaeological sites in Bangladesh, all used to estimate subsidence. The circles show continuous GNSS sites installed by several groups. Red and pink circles were installed by the Lamont-Doherty Earth Observatory (LDEO) and Dhaka University Earth Observatory (DUEO) (Steckler *et al.*, 2016). The pink sites were installed as campaign monuments near Dhaka or currently inactive continuous sites that are available for reoccupation elsewhere. The blue circles were installed by the Earth Observatory of Singapore (EOS) and Bangladesh Geological Survey (BGS) (Mallick *et al.*, 2019) and the yellow circles by the Survey of Bangladesh. The thin black line outlines the area of InSAR analysis by Higgins *et al.* (2014). Historic sites are shown as light green squares with identifying letters inside. S = Shakher Temple, B = Bibi Beguni and Chunakhola Mosques at Bagherat, D = Doyamayee Temple, all from Sarker *et al.* (2012) with a reanalysis of the Shakher Temple in this paper. K = the Katka salt kilns (Hanebuth *et al.*, 2013). W = Wari Bateshwar (Jahan, 2010). The blue inverted triangles are RSET sites. The dark green triangles are tide and river gauges, with the slightly larger symbols showing the sites with data available from the Permanent Service for Mean Sea Level (PSMSL). GNSS and RSET to be installed in July–August 2019 are given by the smaller, paler symbols. [Colour figure can be viewed at wileyonlinelibrary.com]

archaeological site was determined through radiocarbon dating of associated mangrove remains and OSL dating of heated salt-production artefacts (Hanebuth *et al.*, 2013), the latter likely OSL sensitized by the heating process and therefore possessing different OSL properties than natural sedimentary deposits. Many more sites in the area have now been discovered, extending the record an additional 1000 years (T. Hanebuth, personal communication, 2018).

Sarker *et al.* (2012) also estimated subsidence rates, using the relative elevation of four historic sites, including two mosques and two Hindu temples (Figure 5). However, the subsidence rates estimated by Sarker *et al.* (2012) are sensitive to the architectural interpretation of the archaeological monuments. For example, subsidence at the Shakher Temple in the Sundarbans, built during the reign of Raja Paratapaditya, the last King of

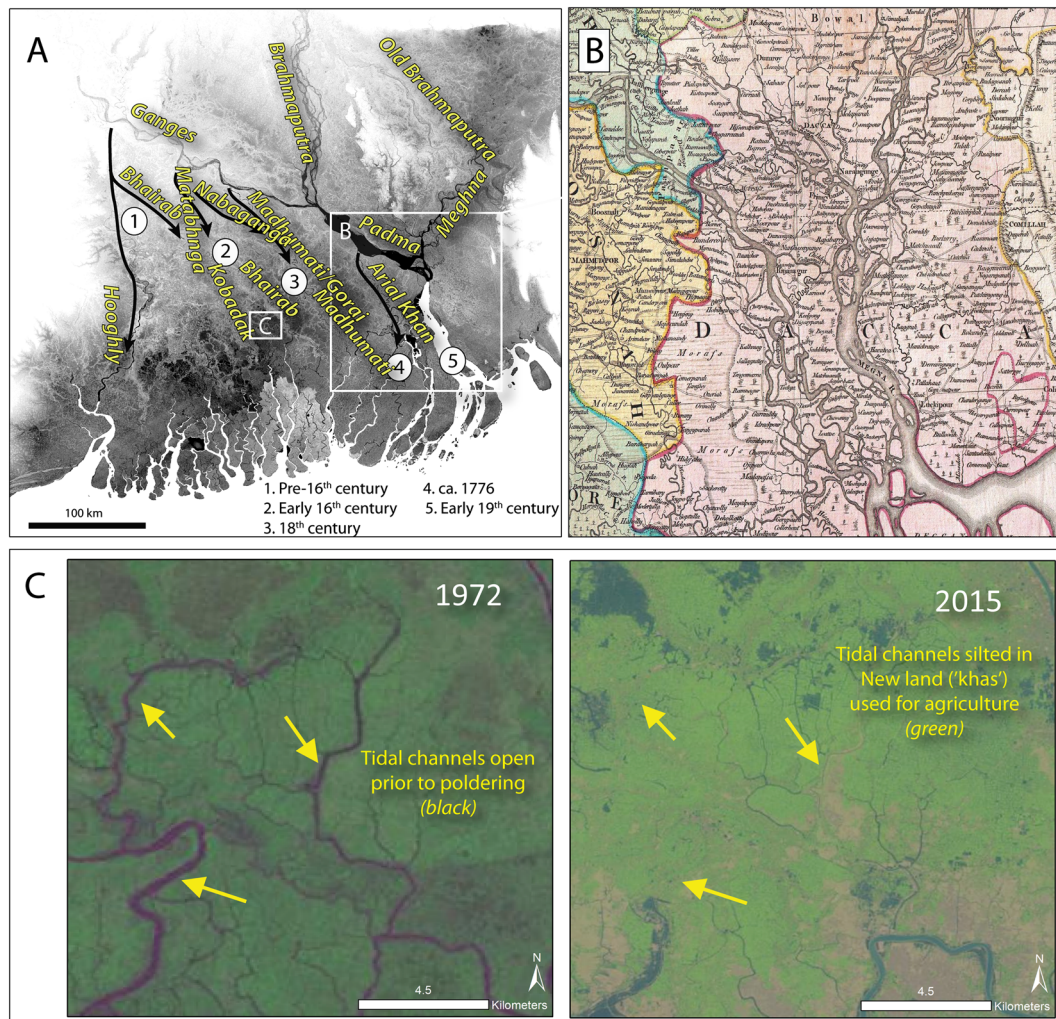


Figure 6. The planform evolution of river and tidal channel networks can be reconstructed over centennial to decadal timescales through the combination of historical map archives and Landsat imagery. (A) River channel migration over the past 400 years is reconstructed from a compilation of historical maps and accounts (Rennell, 1776; Addams Williams, 1919; Brammer, 2004; Best *et al.*, 2007). Black arrows indicate the progressively eastward migration of the Ganges River and distributaries, and relative elevation is shown in greyscale. (B) A portion of one historical map (Rennell, 1776) is shown; note the focus on river channels and village names/locations. (C, from Wilson *et al.*, 2017) Landsat imagery informs rates and patterns of more recent, decadal timescale tidal channel infilling related to human modifications of the delta plain. [Colour figure can be viewed at wileyonlinelibrary.com]

Jessore, before his conquest by the Mughals in 1611 CE, was judged by the present-day elevation of the plinth level (the platform for the building that was constructed to raise it above flood level). Sarker *et al.* (2012) placed this horizon at the entrance of the temple at the top of the stairs, even with the interior of the temple, as is common for Muslim mosques. However, we propose that the plinth level of the Sharker Temple is more likely a lower architectural feature, marked by a ridge in the brickwork at the base of the entrance stairs 0.1 m above the ground and indicating a raised entrance, as is common in Hindu temples. Such discrepancies underscore the need for robust, culturally specific analyses of archaeological sites, and demonstrate that further work is needed to optimize the geoarchaeological record of the Sharker Temple and likely other sites as well.

Historical and satellite-derived maps

Historical maps and accounts in the G-B Delta, while somewhat limited, provide relevant information on landscape changes over the past 400 years (Table I). In particular, historical documents tend to focus on the pathways of the dynamic,

big rivers, while showing less focus on uninhabited regions or unnavigable channels. This reflects the societal importance of rivers as the primary conduits of people and goods until recent engineering advances in transportation. River pathways also dictate the distribution of food resources, both through fisheries and the presence of arable land. As such, the location of towns, obstructions, and the depth/navigability of channels, and defensive positions (for warfare), are often recorded. One example is the highly detailed '1776 Bengal Delta' by Major James Rennell, an engineer for the British East India Company (Figure 6B; Rennell, 1776). It depicts relatively accurate locations and morphology of major river channels, islands, lakes, wetlands, forests, roads, and inhabited towns/villages.

Historical documents also reveal complex landscape occupational histories by the big rivers and their distributaries. For example, Rennell's (1776) map shows that the two mainstem rivers of the G-B Delta had separate distributaries in the late 18th century. Rather than converging to form the Padma River, the Ganges River then occupied a more westward course in what is now the Arial Khan channel, while the Brahmaputra actively flowed down the Old Brahmaputra path into Sylhet Basin (later avulsed into its present channel by 1850 CE; see Best *et al.*, 2007; Pickering *et al.*, 2014).

Additional historical documents, considered in sequence, record the migration of the Ganges River over the past few centuries (Figure 6A), from pre-16th-century occupation of the westward Bhagirathi (now Hooghly) that flowed into Calcutta (now Kolkata) (Addams, 1919; Brammer, 2004), to the more eastward pathway of the Matabhanga/Nabaganga in the early 16th century. Through the 18th century, the Ganges continued its eastward migration, occupying the Madhumati then arriving at the configuration depicted in Rennell's (1776) map (Figure 6B). When the Ganges converged with the Brahmaputra to form the Padma in the early 19th century, locals reported that water from the Ganges was 'dammed back' (leading to up to 2 m increase in water height upstream of the confluence), which forced more water down the secondary older distributaries (Matabhanga, Kumar, Nabaganga, Chitra, Bhairab-Kobadak; Addams, 1919). Subsequently, the modern-day Gorai opened as a relief channel between 1820 and 1840 CE (Addams, 1919; Brammer, 2004), and the older distributaries received less discharge, with flow primarily during the monsoon. At present, those between the Hooghly and Gorai are effectively cut off and fed only by local precipitation (Addams, 1919).

Other information can be obtained from USGS-provided Landsat (modern satellite) images captured approximately every two weeks since 1972. The Landsat record is especially well suited for recording human-induced changes to the Anthropocene delta veneer, due to its historical timescale and spatial resolution (80-m pixel size prior to 1982; 30-m thereafter). Landsat imagery enables planform observations of deltaic change at the mesoscale, for example, infilling of channels in the moribund Ganges Delta plain and channels within the tidal region of the delta (Figure 6C). Such changes have been linked to human modification of channel networks (e.g. Alam, 1996; Pethick and Orford, 2013). Specifically, the construction of embankments in the 1970s to protect >5000 km² of agricultural land (former tidal floodplain) cut off a substantial portion of the tidal prism and more than 1000 linear kilometres of primary creeks, thereby driving siltation and channel infilling in the remaining lower tidal delta channels (Moshin-Uddin and Islam, 1982; Wilson *et al.*, 2017). In the fluvial-dominated section of the delta, scars of former river channels (e.g. oxbow lakes, ridges and swales of scroll and point bar formations) remain prevalent and visible in Landsat imagery, allowing further reconstructions of the paleo-landscape. Clear-sky images, however, are relatively limited to the dry season, and tidal stage is important for landscape change analysis in the tidal delta plain (C. Small, personal communication).

All together, the focus of historic maps on G-B river channel pathways and associated communities, and insights into channel infilling obtained from Landsat imagery, are consistent with a highly bioproductive, densely populated, human-modified, and naturally dynamic landscape. Yet, these records remain intermittently captured snapshots of surface and near-surface changes in the delta and, in the case of historical documents, are subject to human interpretation during the recording process.

Short-Lived Accretion Rate Measurements

Fallout radionuclides have long been used to quantify sediment accretion rates over single-event to decadal time-scales (Table I). ²¹⁰Pb and ¹³⁷Cs are two of the most widely applied of these geochronometers (e.g. He and Walling, 1996; Walling and He, 1997; Hobo, 2015), each being particle reactive and readily sorbing to sediment surfaces. The short-lived fallout radionuclide ⁷Be can be applied to discrete flood events (e.g. Sommerfield *et al.*, 1999) or seasonal sediment deposition

(e.g. Rogers *et al.*, 2013). Other short-term geochronometers can include direct observations of sediment deposition via surface elevation tables and marker horizons (e.g. Day *et al.*, 2011) (Table I). Together these particle tracers (i.e. radionuclides) and direct observations of short-term sedimentation, erosion, and surface elevation comprise an important suite of techniques that bridge the gap between active processes and the stratigraphic record.

Radioisotopes: ⁷Be, ¹³⁷Cs, ²¹⁰Pb

²¹⁰Pb is a naturally occurring radionuclide that has a half-life of 22.5 years and is produced by the decay of its near parent, ²²²Rn gas. ²²²Rn is well mixed in the lower atmosphere and surface ocean, deriving from its parent, ²²⁶Ra, which is widespread in soils, bedrock, and seawater. Thus, as ²¹⁰Pb forms and sorbs to particle surfaces, it becomes an effective tracer for those sediment particles younger than ~4 to 5 half-lives, or up to a century. However, the sorbed nuclides are primarily bound to fine-grained sediments (silts and clays) because of their larger, charged mineral surface, which must be corrected when comparing nuclide concentrations in sands and muds (Goodbred and Kuehl, 1998).

¹³⁷Cs is another radionuclide that is particle reactive and readily sorbs to the surface of sediment particles, making it an effective geochronology tool, but it is not naturally occurring. Rather, ¹³⁷Cs was released to the global atmosphere by above-ground nuclear weapons testing, beginning in the late 1950s until 1963, when the nuclear test-ban treaty was enacted. However, it should be noted that ¹³⁷Cs can be remobilized (i.e. desorb) under strongly reducing conditions, particularly in coarser-grained sediments with weaker bonding sites (Evans *et al.*, 1983).

Compared with the natural production of ²¹⁰Pb via the ²³⁸U decay series, the bomb-produced anthropogenic origin of ¹³⁷Cs yields a very different production history (Figure 7A). Whereas ²¹⁰Pb is produced at a constant but locally variable rate, the production of ¹³⁷Cs principally occurred as a major spike in the middle of the last century. This means that, combined, ²¹⁰Pb and ¹³⁷Cs can provide both a chronostratigraphic horizon and estimates of sediment accumulation rates for ~4 to 6 decades above and below that horizon, under optimal conditions (Figure 7B). However, these results may be complicated by the factors discussed below.

In the Bengal Basin, the concentration profiles of ²¹⁰Pb and ¹³⁷Cs are highly covarying (Figure 7C) – in other words, their accumulation in G-B Delta sediments indicates a similar input history, despite having distinct production rates. To obtain these results, ²¹⁰Pb- and ¹³⁷Cs-tagged sediments must be well mixed in the catchment basin, thereby shredding the signal of their different input histories. This finding reflects the abundant exchange of sediment (i.e. erosion and deposition) between the channel and the floodplain along the fluvial transport pathway (Goodbred and Kuehl, 1998). In other words, the continuous mobilization and mixing of shallow ²¹⁰Pb- and ¹³⁷Cs-tagged sediments with older fluvial sediments both dilutes the concentration of ²¹⁰Pb and ¹³⁷Cs in young deposits and homogenizes the concentration of these tracers. Such a result is consistent with the region's highly mobile braided rivers and tidal channels.

These records also indicate that the input of ²¹⁰Pb- and ¹³⁷Cs-tagged fluvial sediment from the catchment overwhelms local atmospheric deposition and marine production of these radionuclides. This attribute is a direct consequence of the massive sediment load delivered by the Ganges and Brahmaputra Rivers, which serves to dilute local radionuclide

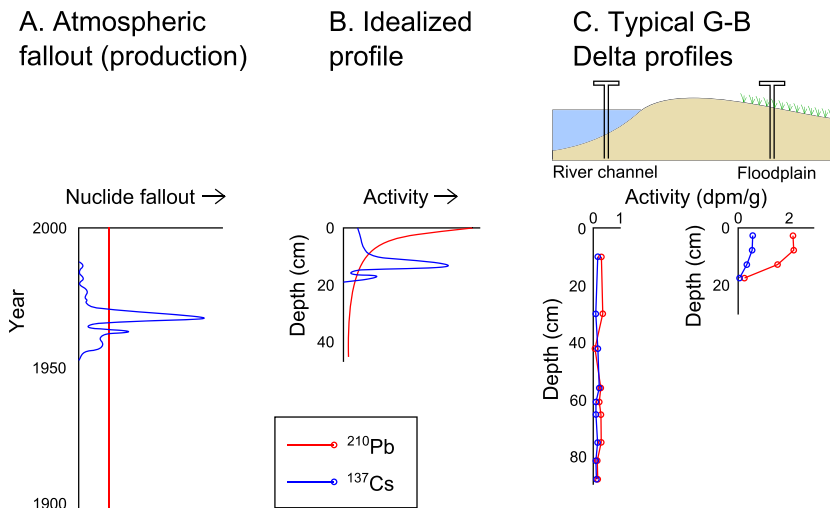


Figure 7. (A) Atmospheric fallout rates, (B) an idealized profile, and (C) typical G-B profiles for ^{210}Pb and ^{137}Cs radionuclides show that, while the production rate and activities in an ideal core are disparate, the activities of these two radionuclides covary in G-B deposits. The atmospheric fallout rate (A) of ^{137}Cs is from Hancock *et al.* (2014). Radionuclide profiles of G-B cores (C) are from Goodbred and Kuehl (1998). [Colour figure can be viewed at wileyonlinelibrary.com]

production and dominate both the depositional history and input of ^{210}Pb and ^{137}Cs to the system.

^7Be is an atmospheric fallout radionuclide formed by the cosmic spallation of nitrogen and oxygen in the upper atmosphere. It is particle reactive and thus a useful sediment tracer (Sommerfield *et al.*, 1999); however, with a 53-day half-life it is only suitable over timescales up to a few months. Thus, ^7Be is often used to track recent river sediment discharge, from that of a single flood event to the seasonal high discharge of a river plume. In the G-B Delta, ^7Be has been applied as a tracer of river-mouth sediments discharged to the inner shelf and advected back onshore by tides (Rogers *et al.*, 2013). Because ^7Be can only be traced for a period of a few months, the presence of this radionuclide in the remote Sundarbans mangrove forest indicates that some of the sediments deposited there originated directly from that year's discharge plume. Based on the concentrations of ^7Be on mangrove sediments compared with those of suspended sediment in the river, it was determined that the fraction of fresh sediment from the river was $\sim 50\%$ of the total deposited (Rogers *et al.*, 2013). As for ^{137}Cs , a comparison of ^7Be and ^{210}Pb concentrations in freshly deposited monsoon sediment proved to be consistent, again reflecting well-mixed sediments derived from the catchment basin.

Although the records of fallout radionuclides (^7Be , ^{137}Cs , ^{210}Pb) in the Bengal Basin generally do not yield typical profiles ideal for estimating changes in accumulation rates with time over recent years to a century (Figure 7C), they have yielded novel insights into mechanisms of sedimentation in the delta. Specifically, these tracers show a consistent pattern of rapid sediment loading across the delta. The persistence of ratios between these tracers, despite their divergent production histories and disparate half-lives, indicates that sediment delivered from the G-B catchments is well mixed by abundant sediment exchange between the channel and the floodplain, leading to a spatially and temporally averaged delivery of nuclide-tagged sediments.

Marker horizons and rod surface elevation tables

Anthropogenically placed surface indicators, called marker horizons (e.g. granular feldspar, coloured sand, brick dust, or even glitter, dispersed typically over 1 m^2 plots) and sediment

collecting plates (tiles, pads, artificial grass mats, or traps, $0.1\text{--}0.5\text{ m}^2$ in size) are physical markers that are placed on the coeval land surface to form a chronologic boundary (Stoddart *et al.*, 1989; Reed *et al.*, 1997; Cahoon *et al.*, 2002). Return visits allow for estimating sedimentation rate since emplacement, by observing the thickness of fresh sediment overlying these noticeable/distinguishable markers. When arranged in arrays or transects, spatial variability of sediment deposition across geomorphic features can be quantified (e.g. Asselman and Middelkoop, 1995).

These short-term measurements are utilized over seasonal or tidal timescales in quiescent wetland or floodplain settings where water velocities are low and sediment accumulation outpaces erosion. They are less effective in high-energy settings where the marker may be washed away. Although granular marker horizons have been shown to remain within the substrate for years to a decade, bioturbation from macro-flora and -fauna can vertically mix the material over time. For these reasons, the sediment plate method is favoured over the granular method in the G-B Delta in regions where crab activity is prevalent (e.g. Sundarbans, unpoldered regions in the tidal delta plain). Sediment plates also offer the advantage of being able to determine the mass and character (i.e. grain size, water/organic content) of accumulated sediment. Yet, sediment plates can likewise be disturbed or lost, especially in regions near human occupation (Rogers and Overeem, 2017). Creative solutions may be adopted to enable plate deployment in human-occupied zones; for example, in the densely populated G-B Delta, plates have been buried below agricultural activity with depth to plate measured using a sounding rod or excavation (Bomer *et al.*, 2017; Wilson *et al.*, 2018).

Marker horizon data are sparse in the G-B Delta and collection has been limited to the past 5–10 years. However, studies from within the Sundarbans mangrove forest (Figure 1) and Meghna estuary have shown that sedimentation rates can be as high as 6 cm over a single monsoon season (Rogers *et al.*, 2013; Rogers and Overeem, 2017), or up to 5 g cm^{-2} (average 1.3 g cm^{-2} ; Rogers *et al.*, 2013). Much of this is from inorganic accumulation ($\sim 97\%$; Rogers *et al.*, 2013) supplied from the sediment-laden rivers that passively flood the landscape by tides and/or riverine floods. These values provide important reference points for comparisons with sedimentation rates in

human-modified portions of the landscape (e.g. polders; Auerbach *et al.*, 2015).

Determining the balance of subsidence and accretion is critical to identifying whether deltas may persist or drown. Rod surface elevation tables (RSETs; Cahoon *et al.*, 2002) have been implemented in deltaic and wetland settings worldwide to measure, with millimetre-scale accuracy, elevation change relative to deep (5–25 m) stainless steel benchmarks (e.g. Day *et al.*, 2011; Webb *et al.*, 2013; Jankowski *et al.*, 2017). Measurements reflect processes acting over seasonal to decadal timescales. If used in conjunction with vertical accretion determinations from marker horizons, net shallow subsidence can also be quantified (Cahoon *et al.*, 2002). While utilization of this method is in its infancy in the G-B Delta (records extend ~5 years; Figure 5), preliminary results of Bomer *et al.* (2017) and Wilson *et al.* (2018) show that the natural surfaces of the Sundarbans are tracking the effective sea-level rise originally postulated by Addams (1919) and documented recently by Pethick and Orford (2013). In addition, polder regions are capable of ameliorating elevation deficits, but only if adequate water and sediment exchange is reinitiated (e.g. Khadim *et al.*, 2013; Haque *et al.*, 2015; Hale *et al.*, 2019). These limited studies demonstrate the potential of RSETs to resolve the sensitive balance between subsidence and accretion in the G-B Delta, and their spatial variability. This information is critical for the sustainable management of the delta (i.e. Bangladesh Planning Commission, 2017), and will be further realized by the expansion of the RSET network in the fluviotidal delta plain over the next decade as part of the greater initiative to improve embankment stability through the Coastal Embankment Improvement Project (Figure 5).

Geodetic Observations

Satellite geodetic observations (Table I) are not geochronologic methods in the traditional sense, yet these instrumental tools fill a niche by providing measurements of landscape change over decadal to event timescales, complementing the tools described above. Here, we discuss the use of the Global Navigation Satellite System (GNSS) and interferometric synthetic aperture radar (InSAR) satellites. In the Bengal Basin, these technologies have mainly been applied to determine tectonic land movement and subsidence. Such research is critical to understanding sedimentation patterns in the Bengal Basin, because of the role tectonics may play in steering river channels (e.g. Akhter, 2010; Grimaud *et al.*, 2017) and generating accommodation (e.g. Johnson and Nur Alam, 1991; Najman *et al.*, 2012).

GNSS

GNSS has expanded beyond the US Global Positioning System (GPS) as Russian (Glonass), EU (Galileo) and Chinese (Beidou/Compass) systems are becoming operational. Positions using the codes broadcast by the satellites have accuracy of a few metres, which can be enhanced to sub-metre accuracy with differential corrections. However, positions using interferometry on the phase of the carrier wave can reach accuracies of ± 2 mm for the horizontal and ± 6 mm for the vertical when processed to provide daily records of land movement. This may improve as more satellites from different systems with different systematic errors become available. GNSS enables observations using fixed antennas over years to estimate rates of tectonic deformation of the crust, as well as its subsidence or uplift, on the order of ± 1 mm year⁻¹ or better. Given the low

signal-to-noise ratio between slow subsidence rates (mm year⁻¹) and the best spatial resolution of several centimetres, it generally takes ~3 years to determine reliable horizontal rates and 5 to 6 years for vertical rates. In particular for the G-B Delta, the large seasonal motions of the ground surface due to loading and unloading of local surface waters, up to 5–6 cm annually (Steckler *et al.*, 2010), make continuous GNSS sites necessary for accurate vertical rates. The first continuous GNSS receivers in Bangladesh were installed in 2003 and the number of sites in the Bengal Basin has grown over the years (Figure 5). Continued measurements will enhance the length of the record and thus the accuracy of subsidence rates.

In Bangladesh, several groups have installed GNSS systems (e.g. Vernant *et al.*, 2014; Reitz *et al.*, 2015; Steckler *et al.*, 2015; Steckler *et al.*, 2016) (Figure 5), returning subsidence rates ranging from <1 to 17 mm year⁻¹ and spatially varying in relation to regional tectonics. Most of the antennas have been mounted on either stainless steel threaded rods cemented or epoxied into reinforced concrete buildings, or on tripods constructed out of welded stainless steel rods driven into the ground. These systems capture subsidence where they are coupled to the ground, either at the foundation of the building or the ~2 m of rods in the ground. Thus, GNSS, particularly of building sites, may not measure the shallowest component of land-surface subsidence (i.e. compaction), thereby underestimating total subsidence. Measurements obtained through fixed monuments may also overestimate land-surface subsidence if the buildings sink under their own weight.

InSAR

This geodetic satellite system uses microwave frequencies in either the L, C or X bands (1.2, 5.3 or 10 GHz) to collect SAR images of the ground surface. The satellite imaging systems look obliquely at the ground (line of sight, LOS) and measure the amplitude and phase of the reflected signal. Differences in the phase represent changes in the travel time of the radar wave and are due to topography in the LOS as well as scattering at the surface and atmospheric delays. Multiple SAR images from different look angles and directions can be combined to create a digital elevation map (DEM). Repeated observations from the same, or almost identical, look angles can be differenced to create an InSAR image that records changes in elevation over time. The phase differences, corrected for geometry and topography, reflect the difference in travel time and thus the distance along the LOS. The phase differences related to the variation in look angle across the images can then be calculated and removed, if precise orbits are known, a process known as interferogram flattening. Ground control from GNSS receivers can help constrain the variation of the phase across the image from orbital errors. The flattened interferogram still has a cyclic change in phase that can be 'unwrapped' by adding the correct number of cycles to yield changes in elevation along the LOS.

A major issue in the Bengal Basin is the coherency of the image. Only coherent patterns of phase can be interpreted. However, scattering at the ground surface by water or vegetation can reduce or eliminate the coherency between pixels, making the use of InSAR in the heavily vegetated Bengal Basin challenging. Over the last two decades, analyses using persistent scatterer techniques to identify networks of individual, phase-coherent targets in a large number of images have been developed. Higgins *et al.* (2014) used the SBAS (small baseline subset) version of the technique with the longer wavelength L-band (23.6 cm) ALOS satellite, which is less affected by vegetation. They still needed to average the interferograms over 16×16 pixels and eliminate images from the monsoon period when

water vapour in the atmosphere is higher. The results showed that subsidence rates vary from 0 to $>18 \text{ mm year}^{-1}$, correlated to subsurface lithology and groundwater extraction (Higgins *et al.*, 2014). At this stage, this is the only published InSAR study of the Bengal Basin (Figure 5). However, multiple efforts are underway using the C-band European Sentinel-1 satellites launched in 2014 and 2016.

Surface Instrumentation

Like geodetic observations, tide gauges and the acoustic Doppler current profiler (ADCP) (Table I) are not traditional geochronology tools, yet these instruments complement traditional approaches by providing high-resolution and contemporary records of fluviodeltaic processes.

Tide gauges

Tide gauges measure changes in absolute water level, with typical temporal resolution ranging from minutes to an hour. Sensors can either be permanent and cabled, or battery-powered and temporary, with individual deployments lasting from days to months. Permanent tide gauges are generally installed as an aid to navigation. Data can be used to understand everything from daily and spring-neap tidal cyclicality, to seasonal patterns, to longer-term subsidence measurements. Finally, an array of tide gauges can provide useful information regarding spatial patterns of water-level change, as they relate to tidal and monsoonal processes.

Tide gauges have been used across southern Bangladesh since at least the 1940s (Pethick and Orford, 2013). Significant logistical challenges associated with using tide gauges in the G-B system relate to the aforementioned inaccessibility of much of the delta plain. Water levels have been monitored along important shipping routes, with little attention paid to the smaller channels. Even if a site is monitored, data fidelity can be a major concern, with data outages or missing metadata as the most common plagues. Furthermore, using tide gauges to compare across space or time requires the use of benchmarks which may be anchored to different depths, experience different degrees of compaction, and therefore capture different components of relative sea-level rise (Keogh and Törnqvist, 2019). This concern is relevant to the G-B system and to deltas in general.

On shorter timescales, tide-gauge data have been used to demonstrate patterns of monsoon-controlled water-level changes, and the importance of inundation frequency on sediment deposition (Hale *et al.*, 2019). (Bain *et al.*, In press) use tide-gauge data in combination with other methods (see ADCP) to demonstrate the complexity of channel interactions on spring-neap timescales, and to help explain observed patterns of changing channel morphology over the past several decades.

On longer timescales, studies have identified trends in sea level as well as tidal amplification due to the construction of polders (e.g. Singh, 2002 ; Pethick and Orford, 2013). Singh (2002) analysed 22 years of tidal data and observed a twofold increase in sea-level rise from west to east, attributed to subsidence. This finding highlights the need for broad spatial coverage in tide-gauge measurements as they relate to subsidence and other processes that may be highly locally variable.

ADCP

ADCP instrumentation measures water velocities at discrete elevations through the water column. Simply put, the instrument emits an acoustic signal (typically 100 kHz to 2 MHz) from each of three to nine acoustic transponders, then records the Doppler shift of the return signal to compute the direction and speed of water movement at distances of $\sim 0.5\text{--}50 \text{ m}$ from the instrument, depending on hardware and deployment configuration. From this, water discharge can be measured in one of two ways. Ship-based measurements are a common method to measure water and sediment discharge across individual tidal cycles (e.g. Mueller and Wagner, 2009 ; Nowacki *et al.*, 2015), whereby the instrument is mounted in a downward-facing orientation to the side of a moving vessel, as it makes repeat channel crossings. Using GPS for location and speed correction, the ADCP measures water velocity throughout the water column at 1 Hz and integrates these measurements to compute water discharge. For longer-term observations, ADCP can be deployed on the seabed in an upward-looking orientation to measure water-column velocities at binned depth intervals. In either deployment mode, observations of water discharge can be complemented by contemporaneous measurements of suspended sediment concentration and used to compute sediment discharge.

With a complex network of channels ranging in widths from metres to kilometres, the G-B Delta offers ample opportunity for ADCP-based measurements. Despite this, there have been relatively few published studies using this method. In the larger channels, ship-based measurements are necessary because of the heterogeneity of tidal current orientation, where one side of the channel may be flooding while the other is ebbing. Furthermore, night-time navigation is unsafe due to unlit boat traffic, making it exceedingly difficult to measure a complete, 12.4-h tidal cycle. Finally, the tidal current velocities can exceed 4 m s^{-1} during spring tides, requiring the vessel to travel through the water at speeds above the manufacturer's recommendation for data fidelity. Deploying instrumentation in smaller channels faces similar constraints, as well as the potential for instrument loss due to a dense population of curious local fishermen.

ADCP have recently been used to interrogate seasonal patterns of water discharge in the southwest delta plain, where tidal variability exerts a stronger control on water discharge than season (Hale *et al.*, 2018). Measurements of instantaneous discharge in a tidal channel in the Shibsra River demonstrate that spring-tide maxima ($>4 \times 10^4 \text{ m}^3 \text{ s}^{-1}$) can exceed the mean annual discharge of the combined Ganges, Brahmaputra, and Meghna Rivers ($\sim 3.8 \times 10^4 \text{ m}^3 \text{ s}^{-1}$). Interestingly, sediment transport in smaller channels demonstrates a more pronounced seasonal signal than in the primary tidal channels (Hale *et al.*, 2018). (Bain *et al.*, In press) demonstrated that these smaller channels are important conduits between the major channels, with the direction of net transport changing with spring-neap tidal variability.

Summary and Challenges

Our review demonstrates the need for careful selection and application of tools, with consideration of the specific research questions and geomorphic characteristics of the field setting. We show that radiocarbon dating in the Bengal Basin is restricted by the availability of suitable organic material, yet, useful ages may be obtained from rare yet isolated organic particles because old-carbon contamination is limited. Luminescence dating is widely applicable to Holocene G-B deposits

if quartz silt is measured, yet, the suitability of sand for dating may be limited by the low sensitivity of immature sediment plus poor bleaching on high-temperature feldspar signals. Archaeological records are valuable but require culturally specific interpretation. GNSS, InSAR, and ADCP technologies are nascent and promising in the Bengal Basin, although they also face challenges associated with monument position, vegetation and river current issues, respectively, as well as record length. Historical documents provide useful yet qualitative and/or incomplete snapshots of human interpretations of the delta, with the focus on river channel pathways and characteristics. Similarly, Landsat gives periodic modern imagery of the planform delta that can be used to infer water and sediment routing and human-induced changes to the delta plain. Marker horizons provide estimates of sediment accretion and, when used in combination with RSETs, can give insight into the balance of subsidence and accretion of the delta plain, albeit over relatively short timescales. Short-lived radionuclides are typically diluted and at low concentrations in the Bengal Basin due to the high sediment load, so that traditional applications are not often possible; however, these tools capture other attributes of the basin, including high sediment flux and basin-scale mixing by the laterally mobile rivers.

This review also reveals shortcomings in the chronologic assessments of the Bengal Basin. Among the methods here, there are none that date deposits beyond 1 million years in age (Figure 8). This hinders chronologic determinations of older regions of the Bengal Basin, such as the Indo-Burman Foldbelt, which is composed of Late Miocene to Pleistocene deposits (see Betka *et al.*, 2018) with poorly defined biostratigraphic markers. The limitations of applying these methods to Pleistocene- to Holocene-aged materials can also be identified. We show that

radiocarbon dating of particulate organic matter may be reliable, yet such ages are often lacking their geologic context. Future work could look at the age offset between radiocarbon ages obtained from particulate organic matter ^{14}C (e.g. Sincavage *et al.*, 2018) and luminescence ages of the deposits in which the particulate organics were embedded. Although luminescence dating is presently underutilized in the Bengal Basin, it is an exciting avenue for future work, which could test the utility of single-grain pIRIR techniques for dating Holocene-aged deposits or applying polymineral indices (e.g. Chamberlain *et al.*, 2017) to trace sediment transport pathways. Among surface processes, fluvial and tidal sediment transport and deposition are spatially and temporally variable across the delta, making the limited observations and challenging working conditions a major constraint. We also anticipate new insights from GNSS, InSAR, SETs, and ADCP as the length and breadth of these records grow.

Looking Forward: Integrating Across Processes and Timescales

Despite some lingering gaps, there have been major advances in Bengal Basin chronologic records and relevant approaches in the past few decades. In essence, the relative dating records of the mid-20th century have been replaced with 'absolute' approaches such as radiocarbon and luminescence dating that give the timing of prehistoric events and allow for calculating rates of geomorphic change. These records can also be supplemented with archaeological analyses and crosschecked to historical documents. New applications of geodetic observations

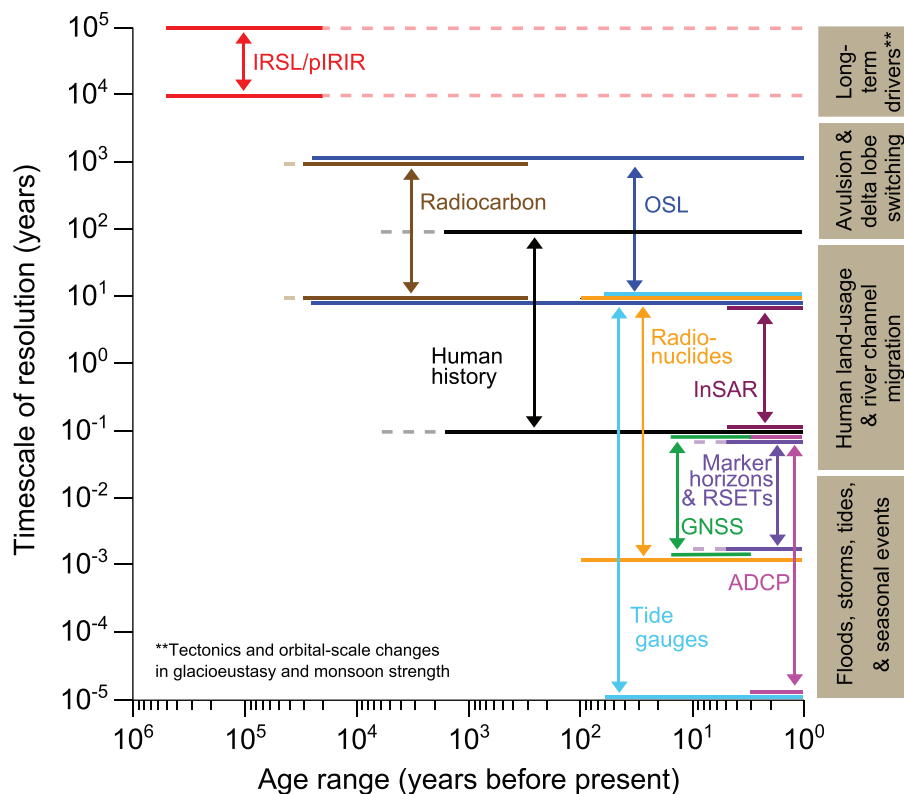


Figure 8. Graph showing the rate resolution and timescale of geochronologic and instrumental methods in the Bengal Basin, and the timescales of processes that drive delta evolution (brown boxes). Darker, solid lines indicate confident age ranges for the methods, and lighter, dashed lines indicate possible age ranges. With a combination of methods, a wide range of timescales and rates can be measured, allowing for integration of the different processes shaping the basin. Present-day is represented on the x-axis as 1 year, although the methods may measure processes operating within the past year (see Table I). [Colour figure can be viewed at wileyonlinelibrary.com]

and surface instrumentation further develop knowledge of delta evolution by quantifying processes acting over decadal to hourly timescales.

Landscapes, and their geologic records, are shaped by events and processes integrated over manifold timescales (e.g. Romans *et al.*, 2016). Having age control across similar timescales thus becomes a requirement to understand their behaviour and evolution. Yet, developing such a database for a large, complex river delta is non-trivial. It necessitates data not only across timescales but also across steep spatial gradients of the continental margin, from fluvial to coastal to marine settings (Figure 2). Thus, developing a truly integrated understanding of the system is an endeavour that can be achieved only through many discrete studies involving experts from a variety of geoscience sub-disciplines. Building on the findings of a few major geologic studies published through to the early 1990s (e.g. Morgan and McIntire, 1959; Coleman, 1969; Umitu, 1993), this paper highlights the great progress made over the last 25 years in developing a large, diverse database that temporally and spatially defines the processes controlling landscape behaviour in the Bengal Basin. With the methodological advancements described herein, it is now possible for the first time to integrate findings across multiple timescales (Figure 8), connecting from process to morphology to stratigraphy. One example is the new ability to connect daily tidal-channel sediment transport (e.g. Hale *et al.*, 2019) with the radionuclide-derived seasonal and decadal-scale deposition (e.g. Allison and Kepple, 2001; Rogers *et al.*, 2013) that defines delta plain response to sea-level change. These landscape-building processes can also be linked to millennial-scale delta lobe construction (e.g. Allison *et al.*, 2003) by constraining the timing of river channel changes through luminescence and radiocarbon dating (e.g. Chamberlain *et al.*, 2017; Sincavage *et al.*, 2018). These large-scale delta lobes become, in turn, the effective stratigraphic units comprising Holocene delta stratigraphy and the complete highstand delta sequence (e.g. Goodbred and Kuehl, 2000a). These results over the last two decades now provide temporal continuity from process to sequence scale. The newest age constraints from feldspar luminescence dating (e.g. Pickering *et al.*, 2017) extend that temporal continuity to the orbital scale by dating deposits back several oxygen isotope stages (Figure 8), making it possible for the first time to investigate how the antecedent template of Late Pleistocene highstand deltas has influenced the development of the Holocene delta and present-day processes of the Anthropocene veneer.

In summary, the nuances of individual geochronologic and instrumental methods reveal attributes of the sedimentary basin, while overlapping geochronologic and instrumental datasets can provide a holistic view of an evolving basin (Figures 2 and 8). The methodological advances outlined here present new opportunities for linking the past and the present, interpreting ongoing processes in the delta in the context of longer-term trends or cycles, and identifying the influence of antecedent geology in Holocene delta morphology. This ever-expanding integration across timescales is generating exciting new opportunities for research.

Acknowledgements—This manuscript was improved through discussions with Paul Betka, Till Hanebuth, Tony Reimann, Chris Small, and Torbjörn Törnqvist. We thank two anonymous reviewers for their constructive comments. Much of the research covered herein has been supported by recent grants from the US National Science Foundation (PIRE #0968354; Belmont Forum #1342946; Coastal SEES #1600319; CNH #1716909), and the Office of Naval Research (#N00014-11-1-0683). Manuscript synthesis was supported in part by National Center for Earth Surface Dynamics (NSF EAR-1246761) and US National

Science Foundation (NSF EAR-1855264) postdoctoral fellowships awarded to Elizabeth Chamberlain Lamont-Doherty Earth Observatory publication number 8346.

References

- Addams WC. 1919. *History of the Rivers in the Gangetic Delta, 1750–1918*. Bengal Secretariat Press: Calcutta.
- Akhter SH. 2010. Earthquakes of Dhaka. In *Environment of Capital Dhaka – Plants, Wildlife, Gardens, Parks, Air, Water and Earthquake*, Hoque S, Karim MA, Mohuya FA (eds). Asiatic Society of Bangladesh: Dhaka; 401–426.
- Alam M. 1996. Subsidence of the Ganges–Brahmaputra Delta of Bangladesh and associated drainage, sedimentation and salinity problems. In *Sea-Level Rise and Coastal Subsidence: Causes, Consequences, and Strategies*, Milliman JD, Haq BU (eds). Springer: Berlin; 169–192.
- Allison M, Kepple E. 2001. Modern sediment supply to the lower delta plain of the Ganges–Brahmaputra River in Bangladesh. *Geo-Marine Letters* **21**(2): 66–74.
- Allison M, Yuill B, Törnqvist T, Amelung F, Dixon TH, Erkens G, Stuurman R, Jones C, Milne G, Steckler M, Syvitski J, Teatini P. 2016. Global risks and research priorities for coastal subsidence. *Eos, Transactions American Geophysical Union* **97**(19): 22–27.
- Allison MA, Khan SR, Goodbred SL, Kuehl SA. 2003. Stratigraphic evolution of the late Holocene Ganges–Brahmaputra lower delta plain. *Sedimentary Geology* **155**: 317–342.
- Anderson E, Libby WF, Weinhouse S, Reid A, Kirshenbaum A, Grosse A. 1947. Radiocarbon from cosmic radiation. *Science* **105**(2735): 576–577.
- Arnold JR, Libby WF. 1949. Age determinations by radiocarbon content: checks with samples of known age. *Science* **110**(2869): 678–680.
- Asselman NE, Middelkoop H. 1995. Floodplain sedimentation: quantities, patterns and processes. *Earth Surface Processes and Landforms* **20**(6): 481–499.
- Auclair M, Lamothe M, Huot S. 2003. Measurement of anomalous fading for feldspar IRSL using SAR. *Radiation Measurements* **37**(4–5): 487–492.
- Auerbach LW, Goodbred SL, Mondal DR, Wilson CA, Ahmed KR, Roy K, Steckler MS, Small C, Gilligan JM, Ackerly BA. 2015. Flood risk of natural and embanked landscapes on the Ganges–Brahmaputra tidal delta plain. *Nature Climate Change* **5**(2): 153–157.
- Azeem M, Khalequzzaman M. 1994. Geology of the southern parts of Khulna and Bagerhat Districts: Bangladesh. Geological Survey of Bangladesh.
- Bain RL, Hale R, Goodbred SL. In press. In review. Flow reorganization in an anthropogenically modified tidal channel network: an example from the southwestern Ganges–Brahmaputra–Meghna Delta. *Journal of Geophysical Research*. <https://doi.org/10.1029/2018JF004996>.
- Bangladesh Planning Commission. 2017. Bangladesh Delta Plan 2100. <http://www.bangladeshdeltaplan2100.org/ganges-barrage-project-blessing-for-country/>.
- Berendsen HJA. 1984. Quantitative analysis of radiocarbon dates of the perimarine area in the Netherlands. *Geologie en Mijnbouw* **63**(4): 343–350.
- Best JL, Ashworth PJ, Sarker MH, Roden JE. 2007. The Brahmaputra–Jamuna River, Bangladesh. In *Large Rivers: Geomorphology and Management*, Gupta A (ed). Wiley: Chichester; 395–430.
- Betka PM, Seeber L, Thomson SN, Steckler MS, Sincavage R, Zoramthara C. 2018. Slip-partitioning above a shallow, weak décollement beneath the Indo-Burman accretionary prism. *Earth and Planetary Science Letters* **503**: 17–28.
- Bomer J, Wilson C, Hale R. 2017. Coupled landscape and channel dynamics in the Ganges–Brahmaputra tidal delta plain, Southwest Bangladesh. In *Proceedings of the AGU Fall Meeting*, abstract #GC14B-07.
- Brammer H. 2004. *Can Bangladesh be Protected from Floods?* The University Press Ltd: Dhakar.
- Brammer H. 2012. *Physical Geography of Bangladesh*. The University Press Ltd: Dhakar.

- Brammer H. 2014. Bangladesh's dynamic coastal regions and sea-level rise. *Climate Risk Management* **1**: 51–62.
- Briant RM, Bateman MD. 2009. Luminescence dating indicates radiocarbon age underestimation in late Pleistocene fluvial deposits from eastern England. *Journal of Quaternary Science* **24**(8): 916–927.
- Briant RM, Brock F, Demarchi B, Langford HE, Penkman KE, Schreve DC, Schwenninger J-L, Taylor S. 2018. Improving chronological control for environmental sequences from the last glacial period. *Quaternary Geochronology* **43**: 40–49.
- Brill D, Reimann T, Wallinga J, May SM, Engel M, Riedesel S, Brückner H. 2018. Testing the accuracy of feldspar single grains to date late Holocene cyclone and tsunami deposits. *Quaternary Geochronology* **48**: 91–103.
- Busschers F, Wesselingh F, Kars R, Versluijs-Helder M, Wallinga J, Bosch J, Timmer J, Nierop K, Meijer T, Bunnik F. 2014. Radiocarbon dating of late Pleistocene marine shells from the southern North Sea. *Radiocarbon* **56**(3): 1151–1166.
- Cahoon DR, Lynch JC, Perez BC, Segura B, Holland RD, Stelly C, Stephenson G, Hensel P. 2002. High-precision measurements of wetland sediment elevation: II. The rod surface elevation table. *Journal of Sedimentary Research* **72**(5): 734–739.
- Chamberlain EL. 2018. A bright approach to geochronology. *Physics Today* **71**(9): 74–75.
- Chamberlain EL, Törnqvist TE, Shen Z, Mauz B, Wallinga J. 2018. Anatomy of Mississippi Delta growth and its implications for coastal restoration. *Science Advances* **4**: eaar4740 <https://doi.org/10.1126/sciadv.aar4740>.
- Chamberlain EL, Wallinga J. 2019. Seeking enlightenment of fluvial sediment pathways by optically stimulated luminescence signal bleaching of river sediments and deltaic deposits. *Earth Surface Dynamics* **7**: 723–736. <https://doi.org/10.5194/esurf-7-723-2019>
- Chamberlain EL, Wallinga J, Reimann T, Goodbred SL, Steckler M, Shen Z, Sincavage R. 2017. Luminescence dating of delta sediments: novel approaches explored for the Ganges–Brahmaputra–Meghna Delta. *Quaternary Geochronology* **41**: 97–111 <https://doi.org/10.5194/esurf-7-723-2019>.
- CIESIN. 2005. Gridded Population of the World, version 3 (GPWv3). NASA Socioeconomic Data and Applications Center (SEDAC): Palisades, NY.
- Coleman JM. 1969. Brahmaputra River: channel processes and sedimentation. *Sedimentary Geology* **3**(2–3): 129–239.
- Cunningham AC, Wallinga J. 2010. Selection of integration time intervals for quartz OSL decay curves. *Quaternary Geochronology* **5**(6): 657–666.
- Cunningham AC, Wallinga J. 2012. Realizing the potential of fluvial archives using robust OSL chronologies. *Quaternary Geochronology* **12**: 98–106.
- Darby SE, Hackney CR, Leyland J, Kumm M, Lauri H, Parsons DR, Best JL, Nicholas AP, Aalto R. 2016. Fluvial sediment supply to a mega-delta reduced by shifting tropical-cyclone activity. *Nature* **539**(7628): 276.
- Day JW, Gunn JD, Folan WJ, Yáñez-Arancibia A, Horton BP. 2007. Emergence of complex societies after sea level stabilized. *Eos, Transactions American Geophysical Union* **88**(15): 169–170.
- Day JW, Kemp GP, Reed DJ, Cahoon DR, Boumans RM, Suhayda JM, Gambrell R. 2011. Vegetation death and rapid loss of surface elevation in two contrasting Mississippi delta salt marshes: the role of sedimentation, autocompaction and sea-level rise. *Ecological Engineering* **37**(2): 229–240.
- Dixon SJ, Smith GHS, Best JL, Nicholas AP, Bull JM, Vardy ME, Sarker MH, Goodbred S. 2018. The planform mobility of river channel confluences: insights from analysis of remotely sensed imagery. *Earth Science Reviews* **176**: 1–18.
- Duller GAT. 2008. Single-grain optical dating of Quaternary sediments: why aliquot size matters in luminescence dating. *Boreas* **37**(4): 589–612.
- Durcan JA, King GE, Duller GA. 2015. DRAC: dose rate and age calculator for trapped charge dating. *Quaternary Geochronology* **28**: 54–61.
- Eaton RM. 1993. *The Rise of Islam and the Bengal Frontier, 1204–1760*. University of California Press: Oakland, CA.
- Evans DW, Alberts JJ, Clark RA, III. 1983. Reversible ion-exchange fixation of cesium-137 leading to mobilization from reservoir sediments. *Geochimica et Cosmochimica Acta* **47**(6): 1041–1049.
- Fisk HN. 1952. *Geological Investigation of the Atchafalaya Basin and the Problem of Mississippi River Diversion*. Vicksburg, MI: Waterways Experiment Station.
- Frazier DE. 1967. Recent deltaic deposits of the Mississippi River: their development and chronology. *Gulf Coast Association of Geological Societies Transactions* **17**: 287–311.
- Gain D, Das SK. 2014. Present status and decreasing causes of shellfish diversity of Passur river, Sundarban, Bangladesh. *Aquaculture, Aquarium, Conservation & Legislation – International Journal of the Bioflux Society* **7**(6): 483–488.
- Galbraith RF, Roberts RG, Laslett GM, Yoshida H, Olley JM. 1999. Optical dating of single and multiple grains of quartz from Jinmium rock shelter, northern Australia: Part I. Experimental design and statistical models. *Archaeometry* **41**(2): 339–364.
- Ganti V, Chu Z, Lamb MP, Nittrouer JA, Parker G. 2014. Testing morphodynamic controls on the location and frequency of river avulsions on fans versus deltas: Huanghe (Yellow River), China. *Geophysical Research Letters* **41**(22): 7882–7890.
- Gao L, Long H, Zhang P, Tamura T, Feng W, Mei Q. 2018. The sedimentary evolution of Yangtze River delta since MIS3: a new chronology evidence revealed by OSL dating. *Quaternary Geochronology* **49**: 153–158.
- Gemmell A. 1988. Zeroing of the TL signal in sediment undergoing fluvio-glacial transport. An example from Austerdalen, Western Norway. *Quaternary Science Reviews* **7**(3–4): 339–345.
- Geyh MA, Roeschmann G, Wijmstra T, Middeldorp A. 1983. The unreliability of ^{14}C dates obtained from buried sandy podzols. *Radiocarbon* **25**(2): 409–416.
- Giosan L, Syvitski J, Constantinescu S, Day J. 2014. Climate change: protect the world's deltas. *Nature News* **516**(7529): 31–33.
- Godfrey-Smith DI, Huntley DJ, Chen WH. 1988. Optical dating studies of quartz and feldspar sediment extracts. *Quaternary Science Reviews* **7**(3–4): 373–380.
- Goodbred SL. 2003. Response of the Ganges dispersal system to climate change: a source-to-sink view since the last interstade. *Sedimentary Geology* **162**: 83–104.
- Goodbred SL, Kuehl SA. 1998. Floodplain processes in the Bengal Basin and the storage of Ganges–Brahmaputra river sediment: an accretion study using ^{137}Cs and ^{210}Pb geochronology. *Sedimentary Geology* **121**: 239–258.
- Goodbred SL, Kuehl SA. 1999. Holocene and modern sediment budgets for the Ganges–Brahmaputra river system: evidence for highstand dispersal to flood-plain, shelf, and deep-sea depocenters. *Geology* **27**: 559–562.
- Goodbred SL, Kuehl SA. 2000a. The significance of large sediment supply, active tectonism, and eustasy on margin sequence development: Late Quaternary stratigraphy and evolution of the Ganges–Brahmaputra delta. *Sedimentary Geology* **133**: 227–248.
- Goodbred SL, Kuehl SA. 2000b. Enormous Ganges–Brahmaputra sediment discharge during strengthened early Holocene monsoon. *Geology* **28**: 1083–1086.
- Goodbred SL, Kuehl SA, Steckler MS, Sarker MH. 2003. Controls on facies distribution and stratigraphic preservation in the Ganges–Brahmaputra delta sequence. *Sedimentary Geology* **155**: 301–316.
- Grall C, Steckler M, Pickering J, Goodbred S, Sincavage R, Paola C, Akhter S, Spiess V. 2018. A base-level stratigraphic approach to determining Holocene subsidence of the Ganges–Meghna–Brahmaputra Delta plain. *Earth and Planetary Science Letters* **499**: 23–36.
- Grimaud JL, Paola C, Ellis C. 2017. Competition between uplift and transverse sedimentation in an experimental delta. *Journal of Geophysical Research: Earth Surface* **122**(7): 1339–1354.
- Guralnik B, Ankjaergaard C, Jain M, Murray AS, Muller A, Walle M, Lowick SE, Preusser F, Rhodes EJ, Wu TS, Mathew G, Herman F. 2015. OSL-thermochronometry using bedrock quartz: a note of caution. *Quaternary Geochronology* **25**: 37–48.
- Hait A, Das J, Ghosh S, Ray A, Saha A, Chanda S. 1996. New dates of Pleisto–Holocene subcrop samples from south Bengal, India. *Indian Journal of Earth Sciences* **23**(1–2): 79–82.
- Hale R, Bain R, Goodbred S, Jr, Best J. 2018. Observations and scaling of tidal mass transport across the lower Ganges–Brahmaputra delta plain: implications for delta management and sustainability. *Earth Surface Dynamics* **7**: 231–245.

- Hale R, Bain R, Goodbred S, Best J. 2019. Seasonal Variability of Forces Controlling Sedimentation in the Sundarbans National Forest, Bangladesh. *Front. Earth Sci.* **7**:211 <https://doi.org/10.3389/feart.2019.00211>.
- Hancock GJ, Tims SG, Fifield LK, Webster IT. 2014. *The Release and Persistence of Radioactive Anthropogenic Nuclides*. Special Publication No. 395. Geological Society: London.
- Hanebuth TJJ, Kudrass HR, Linstädter J, Islam B, Zander AM. 2013. Rapid coastal subsidence in the central Ganges–Brahmaputra Delta (Bangladesh) since the 17th century deduced from submerged salt-producing kilns. *Geology* **41**(9): 987–990.
- Haque KNH, Chowdhury FA, Khatun KR. 2015. Participatory environmental governance and climate change adaptation: mainstreaming of tidal river management in south-west Bangladesh. In *Land and Disaster Management Strategies in Asia*, Ha H (ed). Springer: New Delhi; 189–208.
- He Q, Walling D. 1996. Use of fallout Pb-210 measurements to investigate longer-term rates and patterns of overbank sediment deposition on the floodplains of lowland rivers. *Earth Surface Processes and Landforms* **21**(2): 141–154.
- Higgins SA, Overeem I, Steckler MS, Syvitski JP, Seeber L, Akhter SH. 2014. InSAR measurements of compaction and subsidence in the Ganges–Brahmaputra Delta, Bangladesh. *Journal of Geophysical Research: Earth Surface* **119**(8): 1768–1781.
- Hijma MP, Shen Z, Törnqvist TE, Mauz B. 2017. Late Holocene evolution of a coupled, mud-dominated delta plain–chenier plain system, coastal Louisiana, USA. *Earth Surface Dynamics* **5**(4): 689–710.
- Hobo N. 2015. The sedimentary dynamics in natural and human-influenced delta channel belts. PhD thesis, Utrecht University.
- Huntley DJ, Godfrey-Smith DI, Thewalt MLW. 1985. Optical dating of sediments. *Nature* **313**: 105–107.
- Huntley DJ, Lamothe M. 2001. Ubiquity of anomalous fading in K-feldspars and the measurement and correction for it in optical dating. *Canadian Journal of Earth Sciences* **38**(7): 1093–1106.
- Hütt G, Jaek I, Tchonka J. 1988. Optical dating: K-feldspars optical response stimulation spectra. *Quaternary Science Reviews* **7**(3–4): 381–385.
- Jahan S. 2010. Archaeology of Wari-Bateshwar. *Ancient Asia* **2**: 135–146.
- Jain M, Tandon S. 2003. Fluvial response to Late Quaternary climate changes, western India. *Quaternary Science Reviews* **22**(20): 2223–2235.
- Jain M, Tandon S, Singhvi A, Mishra S, Bhatt S. 2005. Quaternary alluvial stratigraphical development in a desert setting: a case study from the Luni River basin, Thar Desert of western India. *Fluvial Sedimentology* **7**: 349–371.
- Jaiswal MK, Srivastava P, Tripathi JK, Islam R. 2008. Feasibility of the SAR technique on quartz sand of terraces of NW Himalaya: a case study from Devprayag. *Geochronometria* **31**: 45–52.
- Jankowski KL, Törnqvist TE, Fernandes AM. 2017. Vulnerability of Louisiana’s coastal wetlands to present-day rates of relative sea-level rise. *Nature Communications* **8**: 14792.
- Johnson SY, Nur Alam AM. 1991. Sedimentation and tectonics of the Sylhet trough, Bangladesh. *Geological Society of America Bulletin* **103**(11): 1513–1527.
- Joordens JC, D’Errico F, Wesselingh FP, Munro S, De Vos J, Wallinga J, Ankjærsgaard C, Reimann T, Wijbrans JR, Kuiper KF. 2015. Homo erectus at Trinil on Java used shells for tool production and engraving. *Nature* **518**(7538): 228–231.
- Kars R, Wallinga J, Cohen K. 2008. A new approach towards anomalous fading correction for feldspar IRSL dating – tests on samples in field saturation. *Radiation Measurements* **43**(2–6): 786–790.
- Kars RH, Reimann T, Ankjærsgaard C, Wallinga J. 2014. Bleaching of the post-IR IRSL signal: new insights for feldspar luminescence dating. *Boreas* **43**(4): 780–791.
- Keogh ME, Törnqvist TE. 2019. Measuring rates of present-day relative sea-level rise in low-elevation coastal zones: a critical evaluation. *Ocean Science* **15**(1): 61–73.
- Khadim FK, Kar KK, Halder PK, Rahman MA, Morshed AM. 2013. Integrated water resources management (IWRM) impacts in south west coastal zone of Bangladesh and fact-finding on tidal river management (TRM). *Journal of Water Resource and Protection* **5**(10): 953–961.
- Khan SR, Islam B. 2008. Holocene stratigraphy of the lower Ganges–Brahmaputra river delta in Bangladesh. *Frontiers of Earth Science in China* **2**(4): 393.
- Levin I, Heshshaimer V. 2000. Radiocarbon – a unique tracer of global carbon cycle dynamics. *Radiocarbon* **42**(1): 69–80.
- Lindsey EO, Feng L, Hubbard J, Banerjee P, Hill EM. 2019. Active convergence of the India–Burma–Sunda plates revealed by a new continuous GPS network. *Journal of Geophysical Research: Solid Earth* **124**(3): 3155–3171.
- Madsen AT, Buylaert JP, Murray AS. 2011. Luminescence dating of young coastal deposits from New Zealand using feldspar. *Geochronometria* **38**(4): 379–390.
- Madsen AT, Murray AS. 2009. Optically stimulated luminescence dating of young sediments: a review. *Geomorphology* **109**(1–2): 3–16.
- McArthur JM, Ravenscroft P, Banerjee DM, Milsom J, Hudson-Edwards KA, Sengupta S, Bristow C, Sarkar A, Tonkin S, Purohit R. 2008. How paleosols influence groundwater flow and arsenic pollution: a model from the Bengal Basin and its worldwide implication. *Water Resources Research* **44**(11): n/a–n/a. <https://doi.org/10.1029/2007WR006552>.
- McFarlan E, Jr. 1961. Radiocarbon dating of late Quaternary deposits, south Louisiana. *Geological Society of America Bulletin* **72**: 129–158.
- Milliman JD, Farnsworth KL. 2013. *River Discharge to the Coastal Ocean: A Global Synthesis*. Cambridge University Press: Cambridge.
- Morgan JP, McIntire WG. 1959. Quaternary geology of the Bengal Basin, East Pakistan and India. *Geological Society of America Bulletin* **70**(3): 319–342.
- Moshin-Uddin, Md., Islam S. 1982. Polder Development in Bangladesh Paper I: Past and present Development. In: *Polders of the World*, International Institute for Land Reclamation: Netherlands; 288–295.
- Mueller D, Wagner C. 2009. Measuring Discharge with ADCPs from a Moving Boat. US Geological Survey Techniques and Methods 3A-22. USGS: Reston, VA.
- Murray AS, Wintle AG. 2000. Luminescence dating of quartz using an improved single-aliquot regenerative-dose protocol. *Radiation Measurements* **32**(1): 57–73.
- Murray AS, Wintle AG. 2003. The single aliquot regenerative dose protocol: potential for improvements in reliability. *Radiation Measurements* **37**(4–5): 377–381.
- Najman Y, Allen R, Willett E, Carter A, Barfod D, Garzanti E, Wijbrans J, Bickle M, Vezzoli G, Ando S. 2012. The record of Himalayan erosion preserved in the sedimentary rocks of the Hatia Trough of the Bengal Basin and the Chittagong Hill Tracts, Bangladesh. *Basin Research* **24**(5): 499–519.
- Nian X, Zhang W, Wang Z, Sun Q, Chen J, Chen Z. 2018. Optical dating of Holocene sediments from the Yangtze River (Changjiang) Delta, China. *Quaternary International* **467**(B): 251–263.
- Nowacki DJ, Ogston AS, Nittrouer CA, Fricke AT, Van PDT. 2015. Sediment dynamics in the lower Mekong River: transition from tidal river to estuary. *Journal of Geophysical Research: Oceans* **120**(9): 6363–6383.
- Paola C, Twilley RR, Edmonds DA, Kim W, Mohrig D, Parker G, Viparelli E, Voller VR. 2011. Natural processes in delta restoration: application to the Mississippi Delta. *Annual Review of Marine Science* **3**(3): 67–91.
- Pethick J, Orford JD. 2013. Rapid rise in effective sea-level in southwest Bangladesh: its causes and contemporary rates. *Global and Planetary Change* **111**: 237–245.
- Pickering JL, Goodbred SL, Beam JC, Ayers JC, Covey AK, Rajapara HM, Singhvi AK. 2017. Terrace formation in the upper Bengal basin since the Middle Pleistocene: Brahmaputra fan delta construction during multiple highstands. *Basin Research* **30**(S1): 550–567.
- Pickering JL, Goodbred SL, Reitz MD, Hartzog TR, Mondal DR, Hossain MS. 2014. Late Quaternary sedimentary record and Holocene channel avulsions of the Jamuna and Old Brahmaputra River valleys in the upper Bengal delta plain. *Geomorphology* **227**: 123–136.
- Pietsch TJ, Olleya JM, Nanson GC. 2008. Fluvial transport as a natural luminescence sensitiser of quartz. *Quaternary Geochronology* **3**(4): 365–376.
- Rajaguru SN, Deotare BC, Gangopadhyay K, Sain MK, Panja S. 2011. Potential geoarchaeological sites for luminescence dating in the Ganga Bhagirathi–Hugli delta, west Bengal, India. *Geochronometria* **38**(3): 282–291.

- Ramsey CB. 1995. Radiocarbon calibration and analysis of stratigraphy: the OxCal program. *Radiocarbon* **37**(2): 425–430.
- Ray Y, Srivastava P. 2010. Widespread aggradation in the mountainous catchment of the Alaknanda–Ganga river system: timescales and implications to hinterland–foreland relationships. *Quaternary Science Reviews* **29**(17–18): 2238–2260.
- Raymond PA, Bauer JE. 2001. Riverine export of aged terrestrial organic matter to the North Atlantic Ocean. *Nature* **409**(6819): 497.
- Reed DJ, De Luca N, Foote AL. 1997. Effect of hydrologic management on marsh surface sediment deposition in coastal Louisiana. *Estuaries* **20**(2): 301–311.
- Reimann T, Román-Sánchez A, Vanwallegem T, Wallinga J. 2017. Getting a grip on soil reworking – single-grain feldspar luminescence as a novel tool to quantify soil reworking rates. *Quaternary Geochronology* **42**: 1–14.
- Reimann T, Tsukamoto S, Naumann M, Frechen M. 2011. The potential of using K-rich feldspars for optical dating of young coastal sediments – a test case from Darss-Zingst peninsula (southern Baltic Sea coast). *Quaternary Geochronology* **6**(2): 207–222.
- Reimer PJ, Bard E, Bayliss A, Beck JW, Blackwell PG, Bronk Ramsey C, Buck CE, Cheng H, Edwards RL, Friedrich M, Grootes PM, Guilderson TP, Hafliðason H, Hajdas I, Hatté C, Heaton TJ, Hoffmann DL, Hogg AG, Hughen KA, Kaiser KF, Kromer B, Manning SW, Niu M, Reimer RW, Richards DA, Scott EM, Southon JR, Staff RA, Turney CSM, Van der Plicht J. 2013. IntCal13 and Marine13 radiocarbon age calibration curves 0–50,000 years cal BP. *Radiocarbon* **55**(4): 1869–1887.
- Reitz MD, Pickering JL, Goodbred SL, Paola C, Steckler MS, Seeber L, Akhter SH. 2015. Effects of tectonic deformation and sea level on river path selection: theory and application to the Ganges–Brahmaputra–Meghna river delta. *Journal of Geophysical Research: Earth Surface* **120**(4): 671–689.
- Rennell J. 1776. An Actual Survey, of the Provinces of Bengal, Bahar & c. by Major James Rennell Esq. Engineer to the Honorable the East India Company. Published by permission of the Court of Directors from a drawing in their possession by A. Dury.
- Rogers KG, Goodbred SL, Mondal DR. 2013. Monsoon sedimentation on the ‘abandoned’ tide-influenced Ganges–Brahmaputra delta plain. *Estuarine, Coastal and Shelf Science* **131**: 297–309.
- Rogers KG, Overeem I. 2017. Doomed to drown? Sediment dynamics, infrastructure, and the threat of sea level rise in the Bengal Delta. In *Proceedings AGU Fall Meeting*.
- Romans BW, Castellort S, Covault JA, Fildani A, Walsh J. 2016. Environmental signal propagation in sedimentary systems across time-scales. *Earth-Science Reviews* **153**: 7–29.
- Sadler PM. 1981. Sediment accumulation rates and the completeness of stratigraphic sections. *The Journal of Geology* **89**(5): 569–584.
- Saito Y, Wei HL, Zhou YQ, Nishimura A, Sato Y, Yokota S. 2000. Delta progradation and chenier formation in the Huanghe (Yellow River) Delta, China. *Journal of Asian Earth Sciences* **18**(4): 489–497.
- Sarker M, Choudhury G, Akter J, Hore S. 2012. Bengal Delta not sinking at a very high rate. *Daily Star*, 23rd December.
- Sarker MH, Huque I, Alam M, Koudstaal R. 2003. Rivers, chars and char dwellers of Bangladesh. *International Journal of River Basin Management* **1**(1): 61–80.
- Schiffner MB. 1986. Radiocarbon dating and the “old wood” problem: the case of the Hohokam chronology. *Journal of Archaeological Science* **13**(1): 13–30.
- Schokker J, Cleveringa P, Murray AS, Wallinga J, Westerhoff WE. 2005. An OSL dated middle and late quaternary sedimentary record in the Roer Valley Graben (southeastern Netherlands). *Quaternary Science Reviews* **24**(20–21): 2243–2264.
- Shen Z, Tornqvist TE, Mauz B, Chamberlain EL, Nijhuis AG, Sandoval L. 2015. Episodic overbank deposition as a dominant mechanism of floodplain and delta-plain aggradation. *Geology* **43**(10): 875–878.
- Sincavage R, Goodbred S, Pickering J. 2018. Holocene Brahmaputra River path selection and variable sediment bypass as indicators of fluctuating hydrologic and climate conditions in Sylhet Basin, Bangladesh. *Basin Research* **30**(2): 302–320.
- Singh O. 2002. Spatial variation of sea level trend along the Bangladesh coast. *Marine Geodesy* **25**(3): 205–212.
- Small C, Nicholls RJ. 2003. A global analysis of human settlement in coastal zones. *Journal of Coastal Research* **19**(3): 584–599.
- Sohbati R, Jain M, Murray A. 2012. Surface exposure dating of non-terrestrial bodies using optically stimulated luminescence: a new method. *Icarus* **221**(1): 160–166.
- Sommerfield C, Nittrouer C, Alexander C. 1999. ⁷Be as a tracer of flood sedimentation on the northern California continental margin. *Continental Shelf Research* **19**(3): 335–361.
- Spooner NA. 1994. The anomalous fading of infrared-stimulated luminescence from feldspars. *Radiation Measurements* **23**(2–3): 625–632.
- Stanley DJ, Hait AK. 2000. Deltas, radiocarbon dating, and measurements of sediment storage and subsidence. *Geology* **28**(4): 295–298.
- Steckler M, Mondal D, Akhter S, Davis J, Goodbred Jr S, Wilson C, Bulbul M. 2015. Measurements of the balance of subsidence and sedimentation in the coastal zone of Bangladesh. In *Proceedings AGU Fall Meeting*.
- Steckler MS, Akhter SH, Seeber L. 2008. Collision of the Ganges–Brahmaputra Delta with the Burma Arc: implications for earthquake hazard. *Earth and Planetary Science Letters* **273**(3–4): 367–378.
- Steckler MS, Mondal DR, Akhter SH, Seeber L, Feng L, Gale J, Hill EM, Howe M. 2016. Locked and loading megathrust linked to active subduction beneath the Indo-Burman Ranges. *Nature Geoscience* **9**(8): 615.
- Steckler MS, Nooner SL, Akhter SH, Chowdhury SK, Bettadpur S, Seeber L, Kogan MG. 2010. Modeling Earth deformation from monsoonal flooding in Bangladesh using hydrographic, GPS, and gravity recovery and climate experiment (GRACE) data. *Journal of Geophysical Research: Solid Earth* **115**(B8): n/a–n/a <https://doi.org/10.1029/2009JB007018>.
- Stoddart DR, Reed DJ, French JR. 1989. Understanding salt-marsh accretion, Scolt Head Island, Norfolk, England. *Estuaries* **12**(4): 228–236.
- Stokes S, Bray HE, Blum MD. 2001. Optical resetting in large drainage basins: tests of zeroing assumptions using single-aliquot procedures. *Quaternary Science Reviews* **20**(5–9): 879–885.
- Suckow A, Morgenstern U, Kudrass HR. 2001. Absolute dating of recent sediments in the cyclone-influenced shelf area off Bangladesh: comparison of gamma spectrometric (Cs-137, Pb-201, Ra-228), radiocarbon, and Si-32 ages. *Radiocarbon* **43**(2B): 917–927.
- Sugisaki S, Buylaert JP, Murray A, Tada R, Zheng HB, Ke W, Saito K, Chao L, Li SY, Irino T. 2015. OSL dating of fine-grained quartz from Holocene Yangtze delta sediments. *Quaternary Geochronology* **30**: 226–232.
- Thiel C, Buylaert J-P, Murray A, Terhorst B, Hofer I, Tsukamoto S, Frechen M. 2011. Luminescence dating of the Stratzing loess profile (Austria) – testing the potential of an elevated temperature post-IR IRSL protocol. *Quaternary International* **234**(1–2): 23–31.
- Thomsen KJ, Murray AS, Jain M, Botter-Jensen L. 2008. Laboratory fading rates of various luminescence signals from feldspar-rich sediment extracts. *Radiation Measurements* **43**(9–10): 1474–1486.
- Törnqvist TE, González JL, Newsom LA, Van der Borg K, De Jong AFM, Kurnik CW. 2004. Deciphering Holocene sea-level history on the U. S. Gulf Coast: a high-resolution record from the Mississippi Delta. *Geological Society of America Bulletin* **116**: 1026–1039.
- Törnqvist TE, Kidder TR, Autin WJ, Van der Borg K, De Jong AFM, Klerks CJW, Snijders EMA, Storms JEA, Van Dam RL, Wiemann MC. 1996. A revised chronology for Mississippi River subdeltas. *Science* **273**: 1693–1696.
- Törnqvist TE, Rosenheim BE, Hu P, Fernandez AB. 2015. Radiocarbon dating and calibration. In *Handbook of Sea-Level Research*, Shennan I, Long AJ, Horton BP (eds). Wiley: Chichester; 349–360.
- Umitsu M. 1993. Late Quaternary sedimentary environments and landforms in the Ganges Delta. *Sedimentary Geology* **83**(3–4): 177–186.
- Van der Plicht J, Beck JW, Bard E, Baillie MGL, Blackwell PG, Buck CE, Friedrich M, Guilderson TP, Hughen KA, Kromer B, McCormac FG, Bronk Ramsey C, Reimer PJ, Reimer RW, Remmele S, Richards DA, Southon JR. 2004. NotCal04-comparison/calibration ¹⁴C records 26–50 cal kyr BP. *Radiocarbon* **46**: 1225–1238.
- Vernant P, Bilham R, Szeliga W, Drupka D, Kalita S, Bhattacharyya A, Gaur V, Pelguy P, Cattin R, Berthet T. 2014. Clockwise rotation of the Brahmaputra Valley relative to India: tectonic convergence in the eastern Himalaya, Naga Hills, and Shillong Plateau. *Journal of Geophysical Research: Solid Earth* **119**(8): 6558–6571.
- Walling D, He Q. 1997. Use of fallout ¹³⁷Cs in investigations of overbank sediment deposition on river floodplains. *Catena* **29**(3–4): 263–282.

- Wallinga J. 2002. Optically stimulated luminescence dating of fluvial deposits: a review. *Boreas* **31**(4): 303–322.
- Wallinga J, Cunningham AC. 2015. Luminescence dating, uncertainties and age range. In *Encyclopedia of Scientific Dating Methods*, Rink WJ, Thompson JW (eds). Springer: Dordrecht; 440–445.
- Webb EL, Friess DA, Krauss KW, Cahoon DR, Guntenspergen GR, Phelps J. 2013. A global standard for monitoring coastal wetland vulnerability to accelerated sea-level rise. *Nature Climate Change* **3**(5): 458.
- Weinman B, Goodbred SL, Zheng Y, Aziz Z, Steckler M, van Geen A, Singhvi AK, Nagar YC. 2008. Contributions of floodplain stratigraphy and evolution to the spatial patterns of groundwater arsenic in Araihasar, Bangladesh. *Geological Society of America Bulletin* **120**(11–12): 1567–1580.
- Wilson C, Bomer J, Hale R. 2018. Is the Ganges–Brahmaputra Delta drowning? Elevation and sediment dynamics in the natural and human altered tidal delta plain. In *Proceedings AGU Fall Meeting*.
- Wilson CA, Goodbred SL. 2015. Construction and maintenance of the Ganges–Brahmaputra Meghna delta: linking process, morphology, and stratigraphy. *Annual Review of Marine Science* **7**: 67–88.
- Wilson CA, Goodbred SL, Small C, Gilligan JM, Sams S, Mallick B. 2017. Widespread infilling of tidal channels and navigable waterways in human-modified tidal delta plain of southwest Bangladesh. *Elementa: Science of the Anthropocene* **5**: 1–12.
- Wintle AG, Murray AS. 2006. A review of quartz optically stimulated luminescence characteristics and their relevance in single-aliquot regeneration dating protocols. *Radiation Measurements* **41**(4): 369–391.
- Woodroffe CD, Rogers K, McKee KL, Lovelock CE, Mendelssohn I, Saintilan N. 2016. Mangrove sedimentation and response to relative sea-level rise. *Annual Review of Marine Science* **8**: 243–266.